HELSINKI UNIVERSITY OF TECHNOLOGY
Department of Engineering Physics and Mathematics

Miia Hermelin

DEFORMATION OF A THIN SHELL UNDER A CONCENTRATED LOAD

Licentiate's Thesis

Supervisor: Professor Juhani Pitkäranta
Instructor: Professor Juhani Pitkäranta

Helsinki, 29th May, 2005

Tekijä:	Miia Hermelin
Osasto:	Teknillisen fysiikan ja matematiikan osasto
Pääaine:	Matematiikka
Sivuaine:	Mekaniikka
Työn nimi:	Ohuen kuoren muodonmuutos keskitetyn kuorman alla
Title in English:	Deformation of a thin shell under a concentrated load
Professuurin koodi ja nimi:	Mat-1 Matematiikka
Työn valvoja:	Professori Juhani Pitkäranta
Työn ohjaaja:	Professori Juhani Pitkäranta

Tiivistelmä:

Tässä työssä on tutkittu pallosymmetrisen kuoren käytöstä, kun siihen kohdistetaan pistemäinen voima eli keskitetty kuorma. Kuori oletetaan ohueksi, eli sen paksuus oletetaan paljon pienemmäksi kuin sen muut mitat, esimerkiksi kaarevuussäde. Tällöin voimme tutkia kuoren käytöstä lineaarisen kuorimallin avulla. Yhtälöt pyritään ratkaisemaan tarkasti niin pitkälle kuin mahdollista.

Käytettyjä kuorimalleja on kolme: kalvoteoria, Koiter ja Naghdi. Näistä kalvoteoriassa kuoren paksuus oletetaan nollaksi. Koiterin malli on “perinteinen” kuorimalli siinä mielessä, että siinä energia pysyy rajoitettuna eikä leikkausjännityksiä huomioida. Näin saadut muodonmuutokset pysyvät rajoitettuna myös origossa, jossa keskitetyn kuorman vaikutus on suurin.

Naghdin mallissa leikkausjännitykset huomioidaan eikä energia pysy enää rajoitettuna. Näinollen myöskään muodonmuutokset eivät ole origossa rajoitettuja, vaan niissä todetaan olevan logaritminen singulariteetti. Kuorimallien lisäksi työn alussa tutustutaan kahteen laattamalliin: Kirchhoffin ja Reissner-Mindlinin malleihin. Näistä ensinmainittu muistuttaa käytökseltään Koiterin mallia ja jälkimmäinen Naghdin mallia. Laattamallien ratkaisukeinoja voidaan siten käyttää hyväksi haettaessa kuorimallien ratkaisuja.

Muodonmuutosten lisäksi malleista tutkitaan myös niiden lukkiutumista numeerisessa ratkaisussa sekä tähän liittyviä reunahäiriöitä. Työssä ratkaistaan myös sekä Koiterin että Naghdin mallit elementtimenetelmän mukaisella numeerisella ratkaisimella. Saatujen approksimaatioiden voidaan todeta noudattelevan laskettujen tarkkojen ratkaisujen käytöstä.

Sivumäärä: 59 — Avainsanat: FEM, elementtimenetelmä, ohut kuori, Naghdi, Koiter, muodonmuutos, lukkiutuminen, reunahäiriö

Täytetään osastolla

Hyväksytty: Kirjasto:

Helsinki University of Technology — Abstract of Licentiate's thesis
Department of engineering physics and mathematics

Author:	Miia Hermelin	
Department:	Department of engineering physics and mathematics	
Major subject:	Mathematics	
Minor subject:	Mechanics	
Title:	Deformation of a thin shell under a concentrated load	
Title in Finnish:	Ohuen kuoren muodonmuutos keskitetyn kuorman alla	
Chair:	Mat-1 Mathematics	
Supervisor:	Professor Juhani Pitkäranta	
Instructor:	Professor Juhani Pitkäranta	

Abstract:

In this work a radially symmetric shell under a concentrated force is studied. The shell is called shallow if its thickness is assumed to be smaller than its other dimensions, for example the radius of curvature. Then the behaviour of the shell can be studied with linear shell models, as was done in this work. The solutions for the deformations are solved as accurately as possible.

Three different shell models are used: The membrane theory, Koiter's and Naghdi's models. In the membrane theory, the thickness of the shell is assumed to be zero. Koiter's model can be called "classical" since the energy is bounded and there are no shearing strains. Hence, the deformations are bounded even in the origin where the normal deflection gaines its maximum because of the concentrated load.

Naghdi's model includes the shearing strains and hence, the energy is not bounded anymore. Therefore, the deformations are not bounded but they have logarithmic singularity. Two plate models are also studied in this work: Kirchhoff's and Reissner-Mindlin's models. They resemble the Koiter and Naghdi models, respectively. Thus, the methods for finding their solutions are used in solving the shell models.

In addition to the deformations, the locking of the model when solved by a numerical method and the layers involved are examined. A Finite Element Method solver is used both on Koiter's and Naghdi's models. The numerical solutions can be seen to be similar to the exact solutions.

Number of pages: 59	Keywords:	FEM, Finite Element Method, shallow shell, Naghdi, Koiter,deformation, locking, layers

Department fills

Approved:	Library code:

Preface

Writing and studying the subject of this thesis has been very educational as well as interesting. Therefore I would like to thank Juhani Pitkäranta for encouragement and advice concerning this work. Further, I wish to express my gratefulness for Olavi Nevanlinna for the opportunity to do this thesis here at the Institute of Mathematics.

I am also grateful for the help given me by my colleagues at the Institute of Mathematics. Ville Havu and Harri Hakula gave me advice that was both logical and fascinating. Kenrick Bingham was always ready to give a cup of knowledge for a neighbour. I thank my parents for their support and enthusiasm. Finally, I thank my husband Kimmo for parsing, ideas and inspiration.

Engage.

Helsinki, 29th May, 2005

Miia Hermelin

Contents

Chapter 1

Introduction

When an engineer wants to build a bridge or a roof for a hall he needs to know how the elements of the construction behave when subjected to a load, for example wind or snow. This means that he wants to know how much the structure will deform. He might also want to know what kind of a structure would perform best under a specific load. For example, if he knows that there will be 50 centimeters of snow on the roof he wants to know what shape the roof should be to sustain such a load.

In most cases, there is no exact way of knowing what the deformation of the structure is. Based on experience and some mathematics one can make models on the behavior of the structure. These models are essentially partial differential equations that usually cannot be solved exactly but an approximate solutions can be obtained by some numerical method, for example Finite Element Method (FEM).

In the Finite Element Method the problem is divided in smaller parts and then the subproblems are solved individually. Then the solutions are combined and the result obtained is – more or less – a good approximation of the real solution. In the roof case, for example, the roof could be divided into triangles with which the partial differential equations would be solved.

The FEM-theory gives some knowledge on the error made in the approximations. However, if one wants to know which of the different numerical methods gives the best solution – or how good the solution is – one should have some reference problem whose solution is really known. This reference problem is called a benchmark.

In this work a simple radially symmetric benchmark problem will be studied. The object will be a segment of a sphere, a spherical cap, whose thickness is very small compared with its radius. The spherical cap will be loaded by a concentrated force, i.e., it will be "pinched with a sharp needle". It will be assumed that the material will not break or rip but it will just deform – infinitely if necessary. This kind of a structure is called a shallow linear shell.

Three different models will be used to study the behaviour of the segment: The membrane theory, the Koiter and the Naghdi shell models. The segment will also be replaced by a circular plate so that the plate and shell models can be compared.

The main goal of this thesis is to solve the different models as accurately as possible. Different methods for finding the solutions have been used before, see [Łuk79] for example. There the solution is found by Fourier transformation. The value of the (two dimensional) integral is calculated approximately. In this work the symmetry of the problem is exploited so that the need for approximations can hopefully be minimized.

The problem will also be solved using FEM to show that the numerical method will indeed converge to the exact solution.

Below, the outline of the thesis is shortly described.

1.1 Thesis outline

In the Chapter 2 the necessary mathematical and physical tools needed to obtain the equations are introduced. The two objects studied in this work, the plates and the shells, will be shortly defined. The different models that define the behavior of the object when subjected to a certain kind of load will be described. The concepts of finite element locking and boundary layers will be briefly studied. The FEM itself will be introduced.

In Chapter 3 the equations describing the two plate models, Kirchhoff and Reissner-Mindlin models, will be formed. The first one is the classical model and the second one includes terms that are discarded in the Kirchhoff's model. The exact solution of the pinched plate problem according to those models will be found.

A special case of the classical shell models, i.e., the membrane theory, will be studied in Chapter 4. In this model the thickness of the shell is assumed to be zero. It will be seen that the model will be different from the Koiter's model in Chapter 5 when we are near the origin where the load is concentrated on. However, after a certain distance the two models are similar.

In Chapter 5 the classical shell model called the Koiter's model will be studied. The differential equations for the model are formed and solved. The solution will be given by Kelvin functions whose properties will be briefly described in Section 5.2.1. Boundary conditions will give a unique solution for Koiter's model. Then the shell's behavior near the origin, its layers and locking will be studied.

The "modern" shell theory, i.e., the Naghdi's model, will be studied in Chapter 6. It will include the terms – strains – that were discarded in Koiter's model.

Bessel functions are needed in the solution and they will be studied briefly in Section 6.2.1. It will be seen that the Koiter's and Naghdi's models will differ near the origin. The difference will depend on the thickness of the shell. Again, far from the origin, the models will behave similarly. The layers and locking will be studied in this case, too.

In Chapter 7 FEM will be used to solve Naghdi and Koiter models. The results will be compared with the exact solutions. The proper choice of element space and structure will shortly be studied. A way to avoid locking will also be introduced.

Finally, the main results of this thesis are summarized in Chapter 8.

Chapter 2

Preliminaries

In this Chapter the main theories needed in this thesis are introduced. In Sections 2.1 to 2.4 the mathematical and physical background for shells (and plates) is introduced. The energy functional needed to construct the partial differential equations that describe the models is defined.

In Section 2.5 we study the layers and locking that arise in numerical solution. In Sections 2.6 and 2.7 we will shortly formulate the existence and uniqueness of the solution of the partial differential equations.

In the last Section we will introduce the Theory of Finite Element Method so that we can later solve our problem numerically.

2.1 General theory of plates and shells

In this work we study thin plates and shells. This means that the (constant) thickness t of the shell (or plate) is small compared to its other dimensions. A good approximation for this is for example [Nov59]

$$\frac{t}{R} \lesssim 0.05, \tag{2.1}$$

where R is the radius of curvature of the middle surface.

A shell (or plate) of thickness t consists of the points of the domain

$$\Omega = \{\mathbf{x} + z\mathbf{e}_n(\mathbf{x}) : \mathbf{x} \in \Gamma_0, -\frac{t}{2} < z < \frac{t}{2}\} \tag{2.2}$$

where Γ_0 is a part of the surface

$$\Gamma = \{\mathbf{x} \in \mathbb{R}^3 : x_1 \in [-L, L], x_2^2 + x_3^2 = \phi(x_1)^2, \phi \in C^\infty[-L, L], \phi > 0\} \tag{2.3}$$

and $\mathbf{e}_n$ is its normal . If $\Gamma_0 = \Gamma$ then Ω is called a shell of revolution. The surface Γ_0 is called the middle surface of the shell. In this work Γ_0 will be formed by cutting a sphere of radius R centered at $(0,0,-h)$, $h < R$ with xy-plane, i.e., it will be a sphere's cap whose bottom lies at xy-plane. The bottom circle's radius will be L. Then x_i can be given in spherical coordinates (R,θ,φ):

$$\begin{aligned} x_1 &= R\cos\theta - h \\ x_2 &= R\cos\varphi\sin\theta \\ x_3 &= R\sin\varphi\sin\theta \\ x_1^2+x_2^2+x_3^2 &= R^2 \\ \phi(x_1)^2 &= R^2 - x_1^2 \\ h^2+L^2 &= R^2 \end{aligned}$$

If we define

$$\omega = \{(\alpha_1,\alpha_2) \,|\, \alpha_1 \in [-L,L],\ \alpha_2 \in [-\pi,\pi]\}$$

and

$$\begin{aligned} \Phi(\alpha_1,\alpha_2) &= (x_1, \phi(x_1)\sin\alpha_2, \phi(x_1)\sin\alpha_2) \\ \alpha_1^2 + x_1^2 &= R^2 \\ \alpha_2 &= \varphi \end{aligned} \tag{2.4}$$

then $\Gamma_0 = \Phi(\omega)$ and we can study the two dimensional surface ω instead of Γ_0. Geometrically, ω is now Γ_0's projection on xy-plane. The coordinates α_1 and α_2 could more generally be any curvilinear coordinates on ω that satisfy equations (2.4). Now, they become polar coordinates if we do one more transformation

$$\omega = \{(\alpha_1,\alpha_2) : r = \alpha_1 \in [0,L],\ \varphi = \alpha_2 \in [0,2\pi]\} \tag{2.5}$$

and let ϕ have negative values (i.e., $\phi(x) = \pm\sqrt{R^2-(x+h)^2}$). We will denote the unit tangent vectors corresponding to coordinates α_1 and α_2 by $\mathbf{e}_1$ and $\mathbf{e}_2$, respectively. The normal tangent vector will be denoted by $\mathbf{e}_n$.

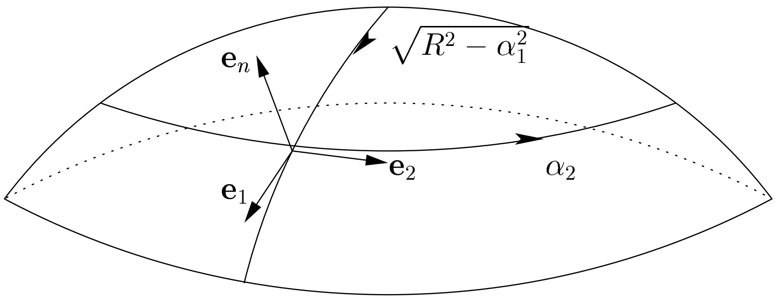

Figure 2.1: A shell of revolution

We will also need the Lamé's coefficients of the surface in polar coordinates:

$$\begin{aligned} A_1 &= 1 \\ A_2 &= r \end{aligned}$$

The curvature tensor of the surface is

$$b_{ij} = \begin{pmatrix} b_{11} & b_{12} \\ b_{21} & b_{22} \end{pmatrix} = \begin{pmatrix} 1/R_1 & 0 \\ 0 & 1/R_2 \end{pmatrix} \tag{2.6}$$

for a radially symmetric plate or shell. It describes the geometrical behavior of the surface. For a plate $b_{11} = b_{22} = 0$ and for the shell that is a part of a sphere whose radius is R, $b_{11} = b_{22} = 1/R$.

If the shell is affected by some load it deforms, i.e., its surface moves and rotates. In practice the load can be caused by wind or snow, for example. In this work we study a theoretical model called the concentrated load. It is a point load acting on one point of the surface. We choose the point of concentration to be the origin, the middle point of the surface to get a symmetric problem. See for Figure 2.2, for example. The direction of the load is chosen to be upwards.

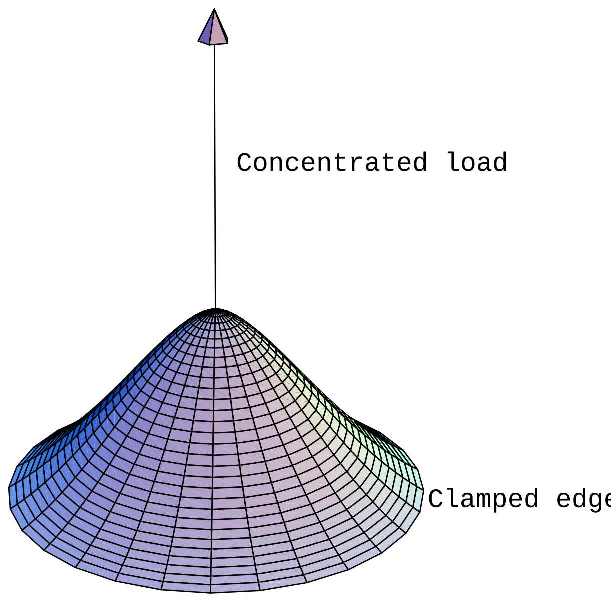

Figure 2.2: A shell of revolution under a concentrated load

The deformation of the shell or plate is generally described by the vector

$$\mathbf{u} = (u, v, w, \theta, \phi)$$

Here u and v are the tangential deformations of the surface and w is the normal deformation. In this work we are mainly interested in w and especially want to know how it behaves near the origin, since the deformation is largest there. The numerical methods used for solving these problems are most vulnerable where the deflection is large so one can see the quality of a method by comparing it's results near the origin to the exact solution gained in this work.

The angular deformations θ and ϕ are the rotations and they describe how the tangents of the lines α_1 and α_2 are rotated around the respective unit vectors $\mathbf{e}_1$ and $\mathbf{e}_2$.

For a plate we have $u = v = \phi = 0$ and for a spherical shell $v = \phi = 0$, because of the symmetry. The deflections can be solved from differential equations which are obtained by varying the energy functional of the plate or shell. The energy consists of membrane, bending and possibly shear strains, which describe the forces acting on and within the object.

For both plates and shells we have two different models. For plates they are the Kirchhoff and Reissner-Mindlin models and for shallow shells they are the Koiter and Naghdi models. The Kirchhoff and Koiter models are the classical models and they assume the transfer shear strains are zero. For these models the rotation is simply $\theta = w'$. The Reissner-Mindlin and Naghdi models are the "modern" models. They include the transfer shear strain in the calculations. The plate models will be more thoroughly studied in Chapter 3, the Koiter model in Chapter 5 and Naghdi model in Chapter 6.

2.2 Strains

The strains describe the behavior of the plate or shell when subjected to a load. The classical models have two strain tensors. The membrane strain tensor β for Koiter and Kirchhoff is

$$\beta_{11} = \frac{1}{A_1}\frac{\partial u}{\partial \alpha_1} + \frac{1}{A_1 A_2}\frac{\partial A_1}{\partial \alpha_2} v + b_{11} w \tag{2.7}$$

$$\beta_{22} = \frac{1}{A_2}\frac{\partial v}{\partial \alpha_1} u + \frac{1}{A_1 A_2}\frac{\partial A_2}{\partial \alpha_1} + b_{22} w \tag{2.8}$$

$$\beta_{12} = \frac{A_1}{2A_2}\frac{\partial}{\partial \alpha_2}\left(\frac{u}{A_1}\right) + \frac{A_2}{2A_1}\frac{\partial}{\partial \alpha_1}\left(\frac{v}{A_2}\right) \tag{2.9}$$

and the bending strain tensor κ is

$$\kappa_{11} = \frac{1}{A_1}\frac{\partial}{\partial \alpha_1}\left(\frac{1}{A_1}\frac{\partial w}{\partial \alpha_1} - b_{11} u\right) + \frac{1}{A_1 A_2}\frac{\partial A_1}{\partial \alpha_2}\left(\frac{1}{A_2}\frac{\partial w}{\partial \alpha_2} - b_{22} v\right) \tag{2.10}$$

$$\kappa_{22} = \frac{1}{A_2}\frac{\partial}{\partial \alpha_2}\left(\frac{1}{A_2}\frac{\partial w}{\partial \alpha_2} - b_{22} v\right) + \frac{1}{A_1 A_2}\frac{\partial A_2}{\partial \alpha_1}\left(\frac{1}{A_1}\frac{\partial w}{\partial \alpha_1} - b_{11} u\right) \tag{2.11}$$

$$\begin{aligned}\kappa_{12} &= \kappa_{21} = \frac{1}{A_1 A_2}\left(\frac{\partial^2 w}{\partial \alpha_1 \partial \alpha_2} - \frac{1}{A_1}\frac{\partial A_1}{\partial \alpha_2}\frac{\partial w}{\partial \alpha_1} - \frac{1}{A_2}\frac{\partial A_2}{\partial \alpha_1}\frac{\partial w}{\partial \alpha_2}\right) \\ &- b_{11}\left(\frac{1}{A_2}\frac{\partial u}{\partial \alpha_2} - \frac{1}{A_1 A_2}\frac{\partial A_1}{\partial \alpha_2} u\right) \\ &- b_{22}\left(\frac{1}{A_1}\frac{\partial v}{\partial \alpha_1} - \frac{1}{A_1 A_2}\frac{\partial A_2}{\partial \alpha_1} v\right)\end{aligned} \tag{2.12}$$

In the classical model the shearing strains were neglected. The Naghdi and Reissner-Mindlin use them and this affects the bending strain which becomes

$$\kappa_{11} = \frac{1}{A_1}\frac{\partial \theta}{\partial \alpha_1} + \frac{1}{A_1 A_2}\frac{\partial A_1}{\partial \alpha_2}\phi - b_{11}\beta_{11} \tag{2.13}$$

$$\kappa_{22} = \frac{1}{A_2}\frac{\partial \phi}{\partial \alpha_2} + \frac{1}{A_1 A_2}\frac{\partial A_2}{\partial \alpha_1}\theta - b_{22}\beta_{22} \tag{2.14}$$

$$\begin{aligned}\kappa_{12} &= \frac{1}{2}\left(\frac{1}{A_2}\frac{\partial \theta}{\partial \alpha_2} + \frac{1}{A_1}\frac{\partial \phi}{\partial \alpha_1}\right) - \frac{1}{2A_1A_2}\left(\frac{\partial A_1}{\partial \alpha_2}\theta - \frac{\partial A_2}{\partial \alpha_1}\phi\right)\\ &- \frac{1}{2}b_{11}\left(\frac{1}{A_2}\frac{\partial u}{\partial \alpha_2} - \frac{1}{2A_1A_2}\left(\frac{\partial A_1}{\partial \alpha_2}u + \frac{\partial A_2}{\partial \alpha_1}v\right)\right)\\ &- \frac{1}{2}b_{22}\left(\frac{1}{A_1}\frac{\partial v}{\partial \alpha_1} - \frac{1}{2A_1A_2}\frac{\partial A_1}{\partial \alpha_2}v\right)\end{aligned} \tag{2.15}$$

The membrane strain tensor β is unaffected. Note that now $\theta \approx w$ only approximately. The shear strain tensor ρ is

$$\rho_1 = -\frac{1}{A_1}\frac{\partial w}{\partial \alpha_1} + b_{11}u + \theta \tag{2.16}$$

$$\rho_2 = -\frac{1}{A_2}\frac{\partial w}{\partial \alpha_2} + b_{22}v + \phi. \tag{2.17}$$

2.3 Energy

The load causes the deformation of the object and hence the object's energy state is altered. The amount of energy depends on the models and can be given by the strains given above. The energy functional $\mathcal{F}$ in general is

$$\mathcal{F}(\mathbf{u}) = \frac{1}{2}\mathcal{A}(\mathbf{u},\mathbf{u}) - \mathbf{f}(\mathbf{u}) \tag{2.18}$$

where $\mathcal{A}$ is the quadratic part of the energy and it represents the deformation energy and $\mathbf{f}$ represents the work done by the external forces. We can further divide $\mathcal{A}$ in two parts:

$$\mathcal{A} = a(\mathbf{u},\mathbf{u}) + t^2 b(\mathbf{u},\mathbf{u})$$

where $a(u,u)$ corresponds to the membrane and – if necessary – shearing energies. The functional $b(u,u)$ corresponds to the bending energy. The energy functional a is given as the integrals

$$\begin{aligned}a(\mathbf{u},\mathbf{u}) = &\int_\omega \nu(\beta_{11}+\beta_{22})^2 + (1-\nu)(\beta_{11}^2 + 2\beta_{12}^2 + \beta_{22}^2)\,\mathrm{d}\omega\\ &+ \gamma(1-\nu)\int_\omega (\rho_1^2+\rho_2^2)\,\mathrm{d}\omega\end{aligned} \tag{2.19}$$

where $\nu \in (0, \frac{1}{2})$ is Poisson's ratio and for simplicity we write $2k = \gamma(1-\nu)$, where γ is a shear correction factor. The first integral is the bending energy and the second is the shear energy which only appears in the Naghdi's and

Reissner-Mindlin's models. For a plate $\beta_{ij} = 0$. The energy b corresponding to the bending strain is

$$b(\mathbf{u}, \mathbf{u}) = \frac{1}{12} \int_\omega (\kappa_{11}^2 + 2\kappa_{12}^2 + \kappa_{22}^2) \, \mathrm{d}\omega. \tag{2.20}$$

If we have $t = 0$ or $\kappa_{ij} = 0$, $i, j \in \{1, 2\}$ for Koiter's model then we have the membrane model which we shall study in detail in Chapter 4.

It will be useful to write the energies as matrix or tensor equations:

$$a(\mathbf{u}, \mathbf{v}) = \int_\omega (\mathbf{S}_\beta \mathbf{u})^T \mathbf{D}_\beta (\mathbf{S}_\beta \mathbf{v}) + (\mathbf{S}_\rho \mathbf{u})^T \mathbf{D}_\rho (\mathbf{S}_\rho \mathbf{v}) \, \mathrm{d}\omega \tag{2.21}$$

where $\mathbf{S}, \mathbf{D} \in \mathbb{R}^{2\times 2}$ and $\mathbf{S}_\rho$ and $\mathbf{D}_\rho$ appear only in the Naghdi's and Reissner-Mindlin's' models. The matrices $\mathbf{S}$ are differential operators and the matrices $\mathbf{D}$ are positive definite. Similarly to a we can write b as

$$b(\mathbf{u}, \mathbf{v}) = \int_\omega (\mathbf{S}_\kappa \mathbf{u})^T \mathbf{D}_\kappa (\mathbf{S}_\kappa \mathbf{v}) \, \mathrm{d}\omega \tag{2.22}$$

The matrices $\mathbf{S}_\beta, \ldots, \mathbf{D}_\kappa$ are defined in Chapter 7 where they are needed to construct the Finite Element Method (FEM) solution. In other parts of the work the equations (2.19) and (2.20) are more useful.

The external forces where given by the linear form $\mathbf{f}(\mathbf{u})$

$$\mathbf{f}(\mathbf{u}) = \int_\omega \mathbf{q} \cdot \mathbf{u} \, \mathrm{d}\omega \tag{2.23}$$

where $\mathbf{q}$ is the traction on the surface of the plate. If we have the above mentioned radially symmetric case, then $\mathbf{q} = P\mathbf{e}_n$ for some constant P and

$$\mathbf{f}(\mathbf{u}) = \int_\omega P w \, \mathrm{d}\omega$$

The constant P determines the magnitude of the load and in this work it is normed by $\int_\omega P \, \mathrm{d}\omega = 1$. In this work we will have a concentrated, symmetric load, hence P is the δ-distribution which we shall study at the end of this Chapter. We have chosen plus-sign in front of δ and have an upward normal deflection. Had we chosen minus-sign, we would have a downward deflection.

2.4 Variational problem

We can now state the exact minimizing problem:

Definition 2.1. For an energy functional $\mathcal{F}$ and some (suitable) energy space V find $\mathbf{u} \in V$ such that

$$\mathcal{F}(\mathbf{u}) \leq \mathcal{F}(\mathbf{v}), \forall \mathbf{v} \in V$$

or find $\mathbf{u} \in V$ such that

$$\mathcal{A}(\mathbf{u}, \mathbf{v}) = \mathbf{f}(\mathbf{v}), \; \forall v \in V$$

With a suitable energy space $V_0 \subset V$, the minimizing problem can be solved uniquely, see Section 2.7. The space V_0 will consist of the kinematically admissible displacement fields with some suitable boundary conditions on $\partial\omega$. We will see that $V = \mathrm{H}^m$ for some $m \in \mathbb{N}$. The spaces H^m are Sobolev-spaces and they are defined later in this Chapter. The choice of m can be justified by both mathematical theory and physically. The (unique) solution $\mathbf{u}$ is the deformation of the shell or plate. The solution can be found by solving the Euler equations (differential equations) given by Method of Variations from $\mathcal{F}$.

In this work the Euler equations are linear and they will be of degree four for plates and six for shells. This means that we will need four and six conditions to determine the unknown constants, respectively, see Table 2.1. For plates we will have two and for shells three boundary conditions. There are several ways of choosing these boundary conditions but in this work we have chosen the so called clamped boundary conditions, i.e., $\mathbf{u}(L) = 0$ and in addition for Kirchhoff's and Koiter's models (since there is no rotation θ involved) we will also demand $w'(L) = 0$. The clamped boundary conditions in the spherically symmetric problem for each of the models can be seen in the Table 2.1. Our

Model	Degrees of Freedom	Boundary conditions
Kirchhoff	4	$w(L) = w'(L) = 0$
Reissner-Mindlin	4	$w(L) = \theta(L) = 0$
Membrane	2	$u(L) = 0$
Koiter	6	$u(L) = w(L) = w'(L) = 0$
Naghdi	6	$u(L) = w(L) = \theta(L) = 0$

Table 2.1: The degrees of freedom and boundary conditions for the models

solutions will then lie in the space

$$V_0 = \{\mathbf{u} \in V : \mathbf{u}(\partial\omega) = 0\}$$

for Naghdi and Reissner-Mindlin and

$$V_0 = \{\mathbf{u} \in V : \mathbf{u}(\partial\omega) = 0, w'(\partial\omega) = 0\}$$

for Koiter and Kirchhoff.

As we can see from Table 2.1, these boundary conditions only solve half of the constants. In all cases, one constant will be determined as the coefficient of the particular solution of the non-homogeneous equations so in fact we will get either three or five undetermined constants from the solutions of the Euler's equations depending on the problem.

If we have no boundary conditions and $\mathbf{q} = 0$ in $\mathcal{F}$ we will get the general solution for the homogeneous Euler's equations. Their solution describes the behaviour of the shell (or plate) with no external fields applied. For a clamped shell, the deformations will vanish.

Determining the rest of the constants will be explained later in Section 2.6, where we will study the energy spaces H^m. Before that, we will shortly study the concept of Layers.

2.5 Layers and locking

Usually, shells deflect the most near the load or the boundary (or both). In this work the deflections near the boundary will be smooth. All the irregularities, if any, lie near the load, i.e., near the origin. The larger the deflections are, the more problems arise when one wants to solve the problem with numerical methods.

The numerical error for a finite element method applied to a shell problem according to [HH96] is

$$e \approx K(d)(h/L)^p. \tag{2.24}$$

Here p is the degree of the approximation (i.e., the degree of the polynomials), h is the mesh size and $d = t/L$ is the length scale of the problem. The function K is determined by the energy functionals of the problem. In [HH96] it is stated that the worst case scenario with

$$K(d) \approx 1/d \tag{2.25}$$

is realized when the problem is bending dominated, i.e., if

$$a(u,u) \leq Ct^2 b(u,u). \tag{2.26}$$

Here a and b are defined in equations (2.19) and (2.20), respectively. If

$$b(u,u) \leq Ca(u,u) \tag{2.27}$$

the problem is called membrane dominated and $K(t)$ is bounded as $t \to 0$ and there may or may not be any locking.

For the bending dominated case, when we have $K(t) \approx 1/t$, we get severe numerical problems as the method converges poorly. This means that the mesh should be refined (i.e., h should be made smaller) very excessively which usually means that the computations become too expensive. This phenomenon is called locking. It was first noted when a shell that was supposed to deform got locked when FEM was applied to it. Hence, the term "locking".

In most cases, the only reasonable way to correct the problem is to heighten the degree p of the solution so that the term $(h/L)^p$ comes smaller. In [HH96] it is stated that $p = 4$ suffices for all problems. However, $p = 3$ may also suffice in certain situations.

When p is increased the locking is removed. Then it is enough to refine the mesh near the singularity. The refinement distance is specified by the dominating layer mode of the problem. The layers are given by the exponential decay of the solution: If the solution has term

$$\exp(-\frac{r}{t^{1/n}}),\ n \in \mathbb{N}$$

in it then it has the scale n . The largest of such n is the dominating layer mode, since all the other modes are inside the area of the dominating mode. The layers can also be found by scaling the problem by $r \to rt^{1/n}$ if no exact solution is available.

When the scaled distance from the origin or boundary is $r \approx 1$, we get an approximation of the solution which does not depend on the thickness parameter t. This mode is connected with the bending dominated locking, since then the refinement of the mesh must be done on the whole shell.

In general, we will have the layer of thickness $r \approx 1$ for both boundary and origin. In [JP01] it is stated that the $n = 1$ mode can only be found in models that have shearing strain involved. Hence, Koiter's model cannot have mode $n = 1$.

The mode $n = 2$ may be seen in all the models. The rest of the modes can only be found in hyperbolic and parabolic problems and our problem (as will be stated in the next Section) is elliptic. Hence, if we have removed the locking, it suffices to refine our mesh within a distance $\approx \sqrt{t}$ from the perturbation which lies in the origin.

2.6 Sobolev spaces and distributions

In this Section we will shortly study the mathematical background of our problem. Since our load will be a distribution (and not a function) our solutions will be calculated in the distributive sense. However, our solutions will finally be "ordinary" functions.

We shall use the standard Sobolev-space notation but for convenience we will briefly repeat it here.

Definition 2.2. The Sobolev space $\mathrm{H}^s(\mathbb{R}^n)$ consists of those functions/distributions u that satisfy

$$(1 + |\xi|^2)^{s/2}\hat{u}(\xi) \in \mathrm{L}^2(\mathbb{R}^n).$$

Here $\hat{u}(\xi)$ is the Fourier transformation of $u(x)$.

Note that $\mathrm{H}^0 = L^2$ and $\mathrm{H}^s \subset \mathrm{H}^t$ when $s > t$. Further,

Theorem 2.3. *If $m \in \mathbb{N}$ then $\mathrm{H}^m(\mathbb{R}^n)$ consists of those functions/distributions whose mth derivatives lie in $\mathrm{L}^2(\mathbb{R}^n)$:*

$$\mathrm{H}^m(\mathbb{R}^n) = \{u \in \mathcal{D}'(\mathbb{R}^n) : D_\alpha u \in \mathrm{L}^2(\mathbb{R}^n)\}.$$

The corresponding norm is then

$$||u||_m = \left(\sum_{k=0}^{m} (D^k u)^2 \right)^{1/2} .$$

The solutions for our problems will lie in some Sobolev spaces. Which one, will be determined with the help of the distribution theory. We will also see that our physical conditions will be satisfied with these energy spaces obtained by the mathematical theory.

Let us next study the properties of some differential equations, the general form of which our Euler equations will obey. Let $\mathcal{L}$ be a linear differential operator of degree N. This means that $\mathcal{L}$ is

$$\mathcal{L} = \sum_{\alpha \leq N} f_\alpha D_\alpha$$

where α is a multi-index and $f_\alpha \in \mathbb{C}$. We also assume that for some $|\alpha| = N$, $f_\alpha \neq 0$. The operator has the characteristic polynomial

$$p(x, y) = \sum_{|\alpha| \leq N} f_\alpha(x) y^\alpha,\ x, y \in \mathbb{R}^n \tag{2.28}$$

and if the polynomial satisfies the condition $p(x, y) \neq 0\, \forall x,\ y \neq 0$ then $\mathcal{L}$ is said to be elliptic.

For example, the Laplace operator

$$\triangle = \frac{\partial^2}{\partial x_1^2} + \cdots + \frac{\partial^2}{\partial x_n^2}$$

is linear and elliptic and its degree is $N = 2$.

The following Theorem will be useful later when we study the energy spaces of our solutions.

Theorem 2.4. *The equation*

$$\mathcal{L} g = f, \quad f \in \mathrm{H}^s,\ s \in \mathbb{R} \tag{2.29}$$

where $\mathcal{L}$ is an elliptic differential operator of order N has a unique solution

$$g \in \mathrm{H}^{N+s}.$$

This is proved for example in [Rud91].

Note that the variational problem defined in Definition 2.1 and satisfying the conditions of Theorem 2.4 gives an elliptic system of differential equations.

The δ-distribution lies in the space $\mathrm{H}^{2'}$ which is the dual space of H^2. We remind that the δ-distribution is a the distribution that satisfies

$$\begin{aligned} \int_\omega \delta \,\mathrm{d}\omega &= 1 \\ \delta &= 0,\, x \neq 0 \end{aligned}$$

or, using the distributions.

$$(f, \delta) := \int_\omega f \delta \,\mathrm{d}\omega = f(0),\, f \in C_0^\infty.$$

The space C_0^∞ is called the test function space. The functions in it are compactly supported and infinitely continuously differentiable. It can be proven that $\delta \in \mathrm{H}^s$ for $s < -3/2$. Hence, $\delta \in \mathrm{H}^{-2} = \mathrm{H}^{2'}$. Thus, the solutions of the non-homogeneous equation (2.29) with $f = \delta$ will be

$$g \in \mathrm{H}^{N-2}.$$

The space H^{N-2} will be the energy space in which our solutions should lie. This condition will determine the rest of the unknown constants of our equations.

2.7 Existence and uniqueness

Let us first note that the energy functional $\mathcal{A} : V \times V \to \mathbb{R}$ is bilinear, i.e., it satisfies

i) $\mathcal{A}(t\mathbf{u}_1 + s\mathbf{u}_2, \mathbf{v}) = t\mathcal{A}(\mathbf{u}_1, \mathbf{v}) + s\mathcal{A}(\mathbf{u}_2, \mathbf{v})$

ii) $\mathcal{A}(\mathbf{u}, t\mathbf{v}_1 + s\mathbf{v}_2) = t\mathcal{A}(\mathbf{u}, \mathbf{v}_1) + s\mathcal{A}(\mathbf{u}, \mathbf{v}_2)$.

Second, it is bounded on $V = \mathrm{H}^m$

$$|\mathcal{A}(\mathbf{u}, \mathbf{v})| \leq C||\mathbf{u}||_m||\mathbf{v}||_m,$$

and so is $f = \delta$

$$|f(\mathbf{u})| = |\mathbf{u}(0)| \leq C||\mathbf{u}||_m.$$

Third, it is elliptic, i.e., it satisfies

$$|\mathcal{A}(\mathbf{u}, \mathbf{u})| \geq C||\mathbf{u}||_m^2, \quad C > 0$$

This can be seen simply by noting that the matrices $\mathbf{D}_\beta, \mathbf{D}_\rho$ and $\mathbf{D}_\kappa$ are positive definite. Hence, the energy functional is positive definite also. The following Theorem is proved for example in [Eva98].

Theorem 2.5. *If operator $\mathcal{A}$ is bounded, bilinear and elliptic on V and if f is bounded on V, then the Problem 2.1 has a unique solution $\mathbf{u} \in V$.*

Since our operators $\mathcal{A}$ and f satisfy all the conditions, our Variational Problem is uniquely solvable. The solution will in practice be calculated from the (elliptic) system of differential equations. If we could not solve them analytically we should solve them approximately. However, the our main goal is to try to solve the equations as accurately as possible.

The problem in this work has been solved before, at least partially, for example in [Łuk79]. The methods have been somewhat different. In [Łuk79], for example, the non-homogeneous part of the Koiter's model has been solved by integration which has then been calculated approximately. In this work we will be able to find the exact solution to the problem as well-known special functions. Approximations will be needed only to enforce the boundary conditions. Some of our methods could probably be applied to more complex cases, too.

2.8 The FEM scheme

The original minimizing problem was stated in Definition 2.1. The FEM-problem is based on finding the minimum for the given energy functional in some subspace V^h (V_0^h) of the original energy space V (V_0). The exact solution $\mathbf{u}$ of the minimum problem will be then replaced by the approximate solution $\mathbf{u}_h$. Our new minimizing problem is then

Definition 2.6. Find $\mathbf{u}_h \in V_0^h \subset V_0$ such that

$$\mathcal{A}(\mathbf{v}, \mathbf{u}_h) = a(\mathbf{v}, \mathbf{u}_h) + t^2 b(\mathbf{v}, \mathbf{u}_h) = \mathbf{f}(\mathbf{v}) \tag{2.30}$$

where a and b are defined by equations (2.21) and (2.22), receptively. The main purpose of FEM is to linearize this minimum problem such that it can be expressed as

$$\mathbf{A}\mathbf{x} = \mathbf{b} \tag{2.31}$$

where $\mathbf{x}$ is an unknown vector, $\mathbf{A}$ is called the stiffness matrix and it corresponds to the quadratic form $\mathcal{A}$. The vector $\mathbf{b}$ corresponds to the load.

The linearization consists of the following main problems:

- Find a suitable mesh, i.e., a way to divide the domain ω in suitable sub-domains.
- Find a suitable element space in which the approximate solution is looked for.

The first problem is not really a problem in this work, since our space is one-dimensional. A simple division of the line segment $[0, L]$ suffices: Let the division of ω be a mesh consisting of points $0 = r_0 < r_1 < \cdots < r_m = L$.

Let $h_k = |r_k - r_{k-1}|$ and let h denote the maximum length $h = \max_k h_k$. Supposedly, $\mathbf{u}_h \to \mathbf{u}$ when $h \to 0$. The speed of the convergence is our main concern.

The second problem should be solved by the energy conditions, i.e., the smoothness of the elements should be determined by the Sobolev space in which the exact solution lies. The locking will however alter the situation so that more complex element functions are needed in some problems. We will define the element space V_h to consist of vectors of some simple and sufficiently smooth functions φ^h (in this work polynomials). The degree of the polynomials is then determined by the degree N of the elliptic problem (see Section 2.6) and the ratio of the bending and straining energies (see Section 2.5). We should choose the polynomials of degree p such that the error

$$e \approx 1/t(h/L)^p$$

becomes reasonably small to avoid the possible locking. If we choose $p = 4$ we get that if $h/L < t^{1/4}$, the problem converges with an acceptable rate. However, we will see that $p = 3$ will suffice. After this the problems with convergence concentrate near the load.

When we have chosen our element functions φ_i^h we can write

$$\mathbf{u} \approx \mathbf{u}_h = \sum_{i=0}^{m} x_i \varphi_i^h$$

for some constants x_i, $i = 0 \ldots m$. Let the vector $\mathbf{x} = (x_0, \ldots, x_m)^T$ and the matrix $\mathbf{N} = (\varphi_0^h, \ldots, \varphi_m^h)$. Then

$$\mathbf{u}_h = \mathbf{N}\mathbf{x}.$$

Let us substitute $\mathbf{u}_h$ in equation (2.30) and write a and b in their matrix forms by equations (2.21) and (2.22). Then by canceling $\mathbf{v}$ that does not depend on ω we get an equation of the desired form (2.31) with

$$\begin{aligned} \mathbf{A} = & \int_\omega (\mathbf{S}_\beta \mathbf{u})^T \mathbf{D}_\beta (\mathbf{S}_\beta \mathbf{v}) + (\mathbf{S}_\rho \mathbf{u})^T \mathbf{D}_\rho (\mathbf{S}_\rho \mathbf{v}) \, \mathrm{d}\omega \\ & + t^2 \int_\omega (\mathbf{S}_\kappa \mathbf{u})^T \mathbf{D}_\kappa (\mathbf{S}_\kappa \mathbf{v}) \, \mathrm{d}\omega \end{aligned} \tag{2.32}$$

and

$$\mathbf{b} = \int_\omega \mathbf{q}\mathbf{N} \, \mathrm{d}\omega \tag{2.33}$$

We want $\mathbf{A}$ to be sparse so we need to choose $\mathbf{N}$ and hence, V_h so that most of the terms of the integral above vanish. This is accomplished by the support condition defined in equation (2.34):

$$\forall k : \operatorname{supp} \varphi_k^h \subset [x_{k-1}, x_{k+1}]. \tag{2.34}$$

After this we can concentrate on our specific problem and try to find its approximate solution. This will be done later in Chapter 7.

Now that the foundation of the mathematical theory on the subject has been laid, the solutions for the problem can be constructed. In the following Chapters both the analytical (as accurately as possible) and numerical solutions are found.

Chapter 3

The circular plate

3.1 Definition of a plate

There are two different models that describe the behavior of the plate. The first one is Kirchhoff's model and it can be subscribed as the classical plate model. The Reissner-Mindlin's model, on the other hand, includes rotations. The energy spaces of these two models also differ: In Kirchhoff's model the normal deformation w is assumed to be in H^2, whereas in Reissner-Mindlin model the normal deflection can have a more singular term in it.

3.2 The Kirchhoff plate

As stated in Chapter 2 the only strain in the Kirchhoff model is the bending strain. Hence, the strain energy functional is

$$\begin{aligned}\mathcal{F}(\mathbf{u}) = \frac{t^2}{24}\int_\omega \nu(\kappa_{11}+\kappa_{22})^2 + (1-\nu)(\kappa_{11}^2+\kappa_{22}^2+2\kappa_{11}\kappa_{22})\,\mathrm{d}\omega \\ - \int_\omega \delta w\,\mathrm{d}\omega.\end{aligned} \tag{3.1}$$

The last term is the effect of the external load concentrated at the origin. The system is then radially symmetric, $u = 0$ and $\mathbf{u} = w\mathbf{e}_n$. The derivatives with respect to $\alpha_2 = \varphi$ are zero in the equation (2.10) so that the bending strain tensor becomes

$$\begin{aligned}\kappa_{11} &= w'' \\ \kappa_{22} &= \frac{w'}{r} \\ \kappa_{12} &= 0.\end{aligned} \tag{3.2}$$

In this classical model, the energy must be finite so that the corresponding strains must lie in L^2. Hence, $w \in \mathrm{H}^2$ which is now our energy space. By the standard Method of Variations applied to the energy in equation (3.1) we get the Euler equation for w:

$$\triangle^2 w = \frac{12}{t^2}\delta. \tag{3.3}$$

Here $\triangle$ is the two-dimensional Laplace-operator, given in radially symmetric polar coordinates:

$$\triangle = \frac{1}{r}\frac{\partial}{\partial r}\left(r\frac{\partial}{\partial r}\right).$$

The homogeneous equation $\triangle^2 w = 0$ gives

$$w = A + Br^2 + Cr^2 \ln r + D \ln r.$$

Since $w \in \mathrm{H}^2$ we must have $D = 0$. The theory of distributions says that

$$w \in \mathrm{H}^{4+s},\ s < -3/2,$$

since the two dimensional δ-distribution lies in $\mathrm{H}^s, s < -3/2$. Hence, $w \in \mathrm{H}^2$ is satisfies the distributive conditions. In the distributive sense

$$\triangle^2(r^2 \ln r) = 8\pi\delta$$

so we must have

$$C = \frac{3}{2\pi t^2}$$

so that the $r^2 \ln r$ term in the homogeneous solution also satisfies the non-homogeneous equation. The coefficients A and B can be solved from the boundary conditions. We have chosen the clamped boundary conditions in this work which means that $w(L) = w'(L) = 0$. Hence, we get that $A = CL^2/2$ and $B = -C(2\ln L + 1)/2$.

We are mostly interested in what happens near the origin. We have:

$$w = \frac{3}{2\pi t^2}\left(r^2 \ln \frac{r}{L} + \frac{L^2 - r^2}{2}\right) \tag{3.4}$$

and when $r \ll 1$,

$$w \approx \frac{3}{2\pi t^2} r^2 \ln r. \tag{3.5}$$

This will also be the most singular term of the Koiter model for shells, as we shall see in Chapter 5. The angular deformation is

$$\theta = w' = \frac{3}{\pi t^2} r \ln \frac{r}{L}. \tag{3.6}$$

Near the boundary, w is bounded and smooth. We shall compare our results with that of the Reissner-Mindlin model which we shall study next.

3.3 The Reissner-Mindlin plate

In the Reissner-Mindlin plate there are both the normal deflection w and the rotation θ involved. In this case the equation $\theta = w'$ applies only approximately. There are either tangential deflections nor other rotations, i.e., $u = v = \phi = 0$, hence, $\mathbf{u} = (\theta, w)$. The energy functional of the Reissner-Mindlin plate model is

$$\begin{aligned}\mathcal{F} = &\frac{k}{2}\int_\omega \rho_1^2 + \rho_2^2 \,\mathrm{d}\omega \\ &+ \frac{t^2}{24}\int_\omega \nu(\kappa_{11}+\kappa_{22})^2 + (1-\nu)(\kappa_{11}^2+\kappa_{22}^2+2\kappa_{12}^2)\,\mathrm{d}\omega - \int_\omega \delta w \,\mathrm{d}\omega.\end{aligned} \tag{3.7}$$

There is no membrane tensor. The bending and the strain tensors are

$$\kappa_{11} = \theta' \tag{3.8}$$

$$\kappa_{22} = \frac{\theta}{r} \tag{3.9}$$

$$\kappa_{12} = 0 \tag{3.10}$$

$$\rho_1 = \theta - w' \tag{3.11}$$

$$\rho_2 = 0. \tag{3.12}$$

Hence, the Method of Variations gives Euler equations for w and θ:

$$k(r\rho_1)' = \delta r \tag{3.13}$$

$$kr\rho_1 + \frac{t^2}{12}(\kappa_{22} + \nu\kappa_{11} - (r(\kappa_{11}+\nu\kappa_{22}))') = 0. \tag{3.14}$$

Here the first equation in (3.13) became from variation with respect to w and the second is from variation with respect to θ. The boundary conditions are now $w(L) = \theta(L) = 0$. We have two boundary condition as in the Kirchhoff's case. However, the energy space is now different: Part of the solution is going to lie in H^2 but the property of the Reissner-Mindlin plate (and also the Naghdi model for shells) is that there is a more singular solution involved. We shall find it by writing

$$w = w_0 + w_1, \quad \theta = \theta_0$$

where we will see that $w_0, \theta_0 \in \mathrm{H}^2$, $w_1 \notin \mathrm{H}^2$ and we will demand $w_1(L) = 0$. Hence, w_0 and θ_0 will be the solutions of the Kirchhoff's model obtained in the previous Section. With these substitutions we get three equations instead of two:

$$-\frac{k}{r}(rw_1')' = \delta \tag{3.15}$$

$$\frac{k}{r}(r(\theta_0 - w_0'))' = 0 \tag{3.16}$$

$$kr(\theta_0 - w_0') + \frac{t^2}{12}\mathcal{G}(\theta_0) = krw_1' \tag{3.17}$$

$$\text{where } \mathcal{G}(\theta) = \frac{\theta}{r} - (r\theta')'. \tag{3.18}$$

Here $\mathcal{G}(\theta)$ is the linear elastic operator for the problem. The solution of the first equation is

$$w_1 = \frac{1}{2\pi k} \ln \frac{r}{L}$$

which is the singular solution we were looking for. Now,

$$w_1 \in \mathrm{H}^{2+s},\ s < -3/2,$$

hence, $w_1 \in \mathrm{H}^0$. Indeed, $\ln r \in \mathrm{H}^0$ (note that we were using polar coordinates). This was the term that was neglected from the Kirchhoff's model because it was too singular. The second and third equation can now be solved to give

$$\begin{aligned} w_0 &= -\frac{A}{k}\ln r + \frac{1}{2}Br^2 - \frac{C}{r^2} + \frac{6}{t^2}(\frac{1}{2\pi} - A)r^2\left(\frac{1}{2}\ln r - \frac{1}{4}\right) + D \\ \theta_0 &= Br + \frac{C}{r} + 6t^2(\frac{1}{2\pi} - A)r\ln r. \end{aligned} \tag{3.19}$$

The equations (3.16) and (3.17) are essentially the same as for the Kirchhoff plate, so the energy condition is $w_0, \theta_0 \in \mathrm{H}^2$ and we get $A = C = 0$. The clamped boundary conditions give the coefficients of the smooth terms

$$B = -\frac{3}{\pi t^2}\ln L$$

and

$$D = \frac{3}{4\pi t^2}L^2$$

so that the final solution is

$$w = w_1 + w_0 \tag{3.20}$$

$$w_1 = -\frac{1}{2\pi k}\ln\frac{r}{L} \tag{3.21}$$

$$w_0 = \frac{3}{2t^2\pi}\left(r^2\ln\frac{r}{L} + \frac{L^2 - r^2}{2}\right) \tag{3.22}$$

$$\theta = \frac{3}{t^2\pi}r\ln\frac{r}{L} \tag{3.23}$$

or, when $r \ll 1$,

$$\begin{aligned} w_1 &\approx -\frac{1}{2\pi k}\ln r \\ w_0 &\approx \frac{3}{2t^2\pi}r^2\ln r \\ \theta &\approx \frac{3}{t^2\pi}r\ln r \end{aligned} \tag{3.24}$$

We see that w_0 is, indeed, the solution of the Kirchhoff's problem. Moreover,

$$\theta_0 = w_0'.$$

The term w_1 is logarithmic so it does not lie in H^2. When t is small, which we assume in this work, the term w_0 will dominate the behaviour of the deflection w and it will start to resemble the Kirchhoff's model. Far from the origin the smooth terms in w_0 become more and more dominating and the difference between Reissner-Mindlin's and Kirchhoff's model becomes negligible. However, near the origin, when t is not negligible, the Kirchhoff's and Reissner-Mindlin's models differ considerably.

Chapter 4

Circular shell membrane theory

The classical Koiter's model will studied in the next Chapter. If we simplify the problem by assuming that $t = 0$ we get the membrane theory. If the shell is loaded in a way that the bending stresses are negligible we may, indeed, assume that $t = 0$ in our shell model. Then the energy will consist of membrane strains only so that

$$\mathcal{A} = a(u, u).$$

Hence the name membrane theory. This condition means that the shell resists stretching, but not bending. For example, a liquid drop would behave in this manner. The error done in this approximation depends mainly on the load and supports of the shell. In the vicinity of a concentrated load the bending strains are not negligible and this simplification does not work. However, far away from the point of the load the membrane theory may be applicable.

In the next Section we will state the Euler equations for the membrane theory problem. In Section 4.2 we will find the solution for the equations. We will also study whether the membrane theory gives a good approximation of our original problem.

4.1 The membrane theory equations

Instead of the concentrated load used in the previous Chapter we will distribute the force along a distance 2ϵ, see Figure 4.1. In order to have the load correctly scaled, it will be defined as

$$P = \begin{cases} P_\epsilon = \frac{1}{\pi\epsilon^2} & , r \leq \epsilon \\ 0 & , r > \epsilon \end{cases}$$

We get the equations of membrane theory by substituting $t = 0$ to equation (2.18) or by assuming that $b(\mathbf{u}, \mathbf{u}) = 0$ and calculating by the Method of Variations. We would get the same equations by substituting $t = 0$ to the

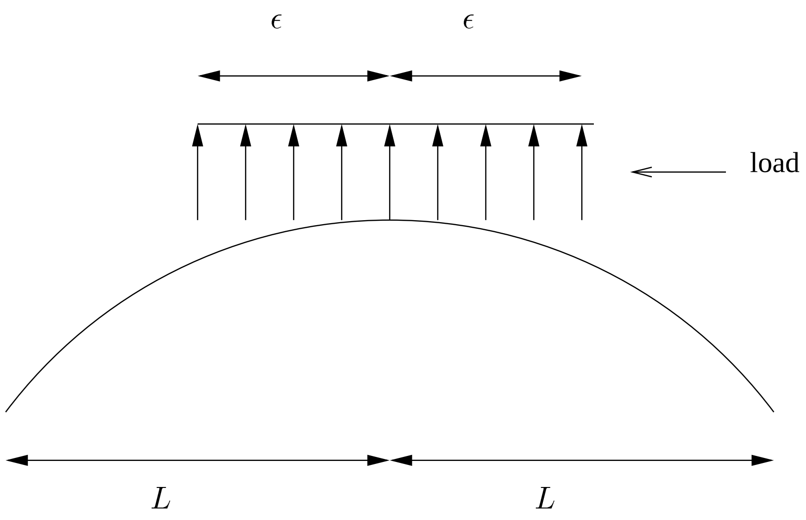

Figure 4.1: The shell under distributed load

Euler equations of the Koiter model (5.3):

$$\begin{aligned} \delta u &: u'' + \frac{u'}{r} + \frac{u}{r^2} + \frac{1+\nu}{R} w' = 0 \\ \delta w &: u' + \frac{u}{r} + \frac{2}{R} w = \frac{R}{1+\nu} P. \end{aligned} \tag{4.1}$$

The integration by parts gives also the following continuity conditions

$$ru' + (1+\nu) r \frac{w}{R} + \nu u \in C \,\text{and}\, u \in C. \tag{4.2}$$

We will use them at $r = \epsilon$. We have also the energy conditions $u \in \mathrm{H}^1$ and $w \in \mathrm{H}^2$ as will be in Koiter's case. Finally, the clamped boundary condition is $u(L) = 0$.

4.2 The membrane theory solution

We see that the solution for the homogeneous equation (4.1) is

$$w = A,\; u = -A\frac{r}{R} + \frac{B}{r}.$$

The particular solution for the non-homogeneous equation is

$$w = \frac{R^2}{2(1+\nu)} P_\epsilon.$$

Let us denote the solution and the corresponding constants by subscripts 1 when $r \leq \epsilon$ and by 2 when $r > \epsilon$. Then, for $r \leq \epsilon$ we get that

$$\begin{aligned} w_1 &= -A_1 R + \frac{R^2}{2(1+\nu)} P_\epsilon \\ u_1 &= A_1 r + \frac{B_1}{r} \end{aligned}$$

The energy condition $u \in \mathrm{H}^1$ then gives $B_1 = 0$. When $r > \epsilon$,

$$\begin{aligned} w_2 &= -A_2 R \\ u_2 &= A_2 r + \frac{B_2}{r}. \end{aligned}$$

The boundary condition $u(L) = 0$ gives $A_2 = -B_2/L^2$. Finally, using the continuity conditions we get

$$\begin{aligned} A_1 &= \frac{P_\epsilon}{2R(\nu-1)}(R^2 - \epsilon^2) \\ A_2 &= -\frac{P_\epsilon}{2R(\nu-1)}\epsilon^2 \\ B_1 &= 0 \\ B_2 &= \frac{P_\epsilon R}{2(\nu-1)}\epsilon^2. \end{aligned}$$

The solution is then

$$w_1 = \frac{1}{2\pi(\nu-1)} + \frac{R^2}{\pi(1-\nu)\epsilon^2} \approx 1/\epsilon^2 \text{ when } \epsilon \to 0 \tag{4.3}$$

$$u_1 = \frac{R^2-\epsilon^2}{2\pi R(\nu-1)\epsilon^2} r \approx r/\epsilon^2 \text{ when } \epsilon \to 0 \tag{4.4}$$

$$w_2 = \frac{1}{2\pi(\nu-1)} \tag{4.5}$$

$$u_2 = \frac{R^2 - r^2}{2\pi(\nu-1)Rr}. \tag{4.6}$$

Note that w_2 and u_2 do not depend on ϵ whereas w_1 and u_1 are singular with respect to ϵ.

We see that $w = w_2$ behaves like a constant when r is large. Near the origin, however, we will see in Chapter 5 that Koiter's solution differs noticeably from the membrane theory. This is because near the origin the bending strain is singular since w is not continuous. Then the strain is not negligible and hence, our original assumption does not apply. When we are far from the origin $w = w_2$ and $\kappa = 0$ so the membrane theory can be used.

Chapter 5

Circular shell Koiter

In this Chapter we will solve the Koiter-model for shallow shells. It is the classical model for shallow shells, since it assumes that the shear strains vanish. Its solution will be finite and smooth. The problem has been solved for example in [Łuk79]. However, the method used in this thesis differs from previous work and we will be using the newer method in the more difficult Naghdi-model in Chapter 6.

5.1 The Koiter shell equations

Our deduction will be much like in Section 3.2. The tangential as well as rotational deflections vanish and we have $\mathbf{u} = (u, \theta, w)$. The energy functional of the Koiter model is

$$\begin{aligned}\mathcal{F}(\mathbf{u}) = \frac{1}{2}\int_\omega \nu(\beta_{11}+\beta_{22})^2 + (1-\nu)(\beta_{11}^2 + 2\beta_{12}^2 + \beta_{22}^2)\, d\omega \\ + \frac{t^2}{24}\int_\omega \nu(\kappa_{11}+\kappa_{22})^2 + (1-\nu)(\kappa_{11}^2 + 2\kappa_{12}^2 + \kappa_{22}^2)\, d\omega - \int_\omega \delta w\, \mathrm{d}\omega\end{aligned} \tag{5.1}$$

where tensors β_{11}, β_{12}, β_{22}, κ_{11}, κ_{12} and κ_{22} are in this spherical case defined by

$$\begin{cases} \beta_{11} = u' + \frac{w}{R} \\ \beta_{12} = 0 \\ \beta_{22} = \frac{u}{r} + \frac{w}{R} \\ \kappa_{11} = w'' \\ \kappa_{12} = 0 \\ \kappa_{22} = \frac{w'}{r} \end{cases} \tag{5.2}$$

Since the energy associated with the strains should be finite we should have the corresponding strains to lie in L^2. Hence, our energy space for w and u are H^2 and H^1, respectively. The Euler equations of the Koiter model by the

Method of Variations are:

$$
\begin{aligned}
\delta u &: \frac{u}{r} - u' - ru'' - (1+\nu)\frac{r}{R}w' = 0 \\
\delta w &: \frac{1+\nu}{R}(ru' + 2\frac{r}{R}w + u) + \frac{t^2}{12}r \triangle^2 w = \delta r
\end{aligned}
\tag{5.3}
$$

Here $\triangle$ is the Laplace's operator given in polar coordinates. The clamped boundary conditions are $u(R) = w(R) = w'(R) = 0$.

5.2 Solving the Koiter equations

The solution of the equations (5.3) will be given by the Kelvin functions. We will study them in the next Section before solving the equations.

5.2.1 Kelvin functions

The general form of a Kelvin equation is

$$x^4 w^{(4)} + 2x^3 w''' - (1+2s^2)(x^2 w'' - xw') + (s^4 - 4s^2 + x^4)w = 0 \tag{5.4}$$

and the solutions are

$$w = \operatorname{ber}_{\pm s} x,\ \operatorname{bei}_{\pm s} x,\ \operatorname{ker}_{\pm s} x,\ \operatorname{kei}_{\pm s} x.$$

We shall be interested in the special case $s = 0$, so that the equation (5.4) is

$$\triangle^2 w + w = 0$$

where $\triangle$ is in polar coordinates. We suppress the subscripts from the solutions in this case: $\operatorname{ber}_0 = \operatorname{ber}$ and so on.

When x is near origin, we have the following series representations for the Kelvin functions:

$$
\begin{aligned}
\operatorname{ber}(x) &= 1 - x^4/64 + \mathcal{O}(x^8) \\
\operatorname{bei}(x) &= x^2/4 - x^6/576 + \mathcal{O}(x^{10}) \\
\operatorname{ker}(x) &= -\ln(\frac{x}{2})\operatorname{ber}(x) + \frac{\pi}{4}\operatorname{bei}(x) + \gamma + \mathcal{O}(x^4) \\
&= -\ln(\frac{x}{2})(1 - x^4/64) + \gamma + \mathcal{O}(x^2) \\
\operatorname{kei}(x) &= -\ln(\frac{x}{2})\operatorname{bei}(x) - \frac{\pi}{4}\operatorname{ber}(x) + \mathcal{O}(x^2) \\
&= -\ln(\frac{x}{2})x^2/4 - \frac{\pi}{4} + \mathcal{O}(x^2)
\end{aligned}
\tag{5.5}
$$

On the other hand if $x \gg 0$ (in Beta [LR99] $x > 10$) we have exponential growth/decrease:

$$
\begin{aligned}
\operatorname{ber}(x) &= \frac{e^{x/\sqrt{2}}}{\sqrt{2\pi x}}\left(\cos\left(\frac{x}{\sqrt{2}} - \frac{\pi}{8}\right) + \frac{1}{8x}\sin\left(\frac{x}{\sqrt{2}} - \frac{3\pi}{8}\right)\right) \\
\operatorname{bei}(x) &= \frac{e^{x/\sqrt{2}}}{\sqrt{2\pi x}}\left(\sin\left(\frac{x}{\sqrt{2}} - \frac{\pi}{8}\right) + \frac{1}{8x}\cos\left(\frac{x}{\sqrt{2}} - \frac{3\pi}{8}\right)\right) \\
\operatorname{ker}(x) &= \frac{e^{-x/\sqrt{2}}}{\sqrt{2\pi x}}\left(\cos\left(\frac{x}{\sqrt{2}} + \frac{\pi}{8}\right) - \frac{1}{8x}\sin\left(\frac{x}{\sqrt{2}} + \frac{3\pi}{8}\right)\right) \\
\operatorname{kei}(x) &= \frac{e^{-x/\sqrt{2}}}{\sqrt{2\pi x}}\left(\sin\left(\frac{x}{\sqrt{2}} + \frac{\pi}{8}\right) + \frac{1}{8x}\cos\left(\frac{x}{\sqrt{2}} + \frac{3\pi}{8}\right)\right)
\end{aligned}
\tag{5.6}
$$

We shall use the following approximations for the derivatives of the Kelvin functions when x is large:

$$
\begin{aligned}
\operatorname{ber}' &= \frac{1}{\sqrt{2}}(\operatorname{ber} - \operatorname{bei}) \\
\operatorname{bei}' &= \frac{1}{\sqrt{2}}(\operatorname{ber} + \operatorname{bei}) \\
\operatorname{ker}' &= -\frac{1}{\sqrt{2}}(\operatorname{ker} + \operatorname{kei}) \\
\operatorname{kei}' &= \frac{1}{\sqrt{2}}(\operatorname{ker} - \operatorname{kei})
\end{aligned}
\tag{5.7}
$$

The following integration formula will also be useful:

$$
\int xf \;\mathrm{d}x = xg', \tag{5.8}
$$

where the functions f and g are any of the pairs

$$
\begin{cases} f = \operatorname{ber}(x) \\ g = \operatorname{bei}(x) \end{cases}
\qquad
\begin{cases} f = \operatorname{bei}(x) \\ g = -\operatorname{ber}(x) \end{cases}
\qquad
\begin{cases} f = \operatorname{ker}(x) \\ g = \operatorname{kei}(x) \end{cases}
\qquad
\begin{cases} f = \operatorname{kei}(x) \\ g = -\operatorname{ker}(x) \end{cases}
\tag{5.9}
$$

More properties of Kelvin functions can be found in Beta [LR99] or Abramovitz [MA65]. In the next section we shall use these properties to solve and analyze the solution of the Koiter-model's Euler equations.

5.2.2 The Koiter solution

First we note that we get two solutions for the equation independent of t:

$$
\mathbf{u}_1 = \begin{pmatrix} u & w \end{pmatrix} = \begin{pmatrix} \frac{F}{r} & 0 \end{pmatrix} \quad \mathbf{u}_2 = A\begin{pmatrix} 1 & -\frac{r}{R} \end{pmatrix} \tag{5.10}
$$

where A and F are some constants. Then we try to find four more solutions – dependent of t – by substituting

$$\hat{u} = u' + \frac{u}{r}$$

to (5.3). We get

$$\delta u \;:\; -\hat{u}' - (1+\nu)\frac{w'}{R} = 0 \tag{5.11}$$

$$\delta w \;:\; \frac{1+\nu}{R}(\hat{u} + 2\frac{w}{R}) + \frac{t^2}{12}\Delta^2 w = \delta \tag{5.12}$$

so we can get from the first equation

$$\hat{u}' = -(1+\nu)\frac{w'}{R}$$

and integrating this we have

$$\hat{u} = -(1+\nu)\frac{w}{R} + \hat{A}, \tag{5.13}$$

where $\hat{A}$ corresponds to the solution $\mathbf{u}_2$ in equation (5.10) so that we can leave it out.

Substituting (5.13) with $\hat{A} = 0$ in the equation (5.12) we get a Kelvin-equation for w. Let us denote its solution by w_K to make the difference between the whole solution and the Kelvin-equations solution. Hence,

$$\triangle^2 w_K + \alpha^4 w_K = \frac{12}{t^2}\delta \tag{5.14}$$

Here the positive constant α is

$$\alpha = (\frac{12(1-\nu^2)}{R^2 t^2})^{1/4}. \tag{5.15}$$

Based on the results from the previous section, we now know that the solution w_K of the homogeneous part of the equation (5.14) is some linear combination of $\mathrm{ber}(\alpha r)$, $\mathrm{bei}(\alpha r)$, $\mathrm{ker}(\alpha r)$ and $\mathrm{kei}(\alpha r)$. Let us denote the (distributive) solution of the non-homegeneous equation (5.14) by w_0. Adding the constant solution of $\mathbf{u}_1$ we get that the whole normal deflection is

$$\begin{aligned} w(r) &= w_K + w_0 + A \\ &= B\,\mathrm{ber}(\alpha r) + C\,\mathrm{bei}(\alpha r) + D\,\mathrm{kei}(\alpha r) + E\,\mathrm{ker}(\alpha r) + A + w_0 \end{aligned} \tag{5.16}$$

where A, B, C, D and E are unknown constants to be determined later.

Since

$$\hat{u} = u' + \frac{u}{r} = -(1+\nu)\frac{w_K}{R} \tag{5.17}$$

we see that

$$u = \frac{1}{r}(\int -(1+\nu)\frac{w_K}{R} r \;\mathrm{d}r + F).$$

Here we get the solution F/r which was already obtained as $\mathbf{u}_1$. Adding $\mathbf{u}_2$ to the solution and using the integration formulas (5.8) we get

$$\begin{aligned} u = &\frac{F}{r} - \frac{A}{R} r \\ &- \frac{1+\nu}{R\alpha^2}(B \operatorname{bei}'(\alpha r) - C \operatorname{ber}'(\alpha r) - D \operatorname{ker}'(\alpha r) + E \operatorname{kei}'(\alpha r)) \end{aligned} \tag{5.18}$$

From the condition $w \in \mathrm{H}^2$ we have $E = 0$. We want to determine a particular solution w_0 of the non-homogeneous equations with the distributive term $\frac{12}{t^2}\delta$. It can be solved by the Fourier transformation. Let us denote by ξ the variable in the Fourier side and the Fourier transformation of w is $\hat{w}$. Then

$$\hat{w}(\xi) = \frac{12}{t^2} \frac{1}{\eta^4 + \alpha^4},$$

where $\eta = |\xi|$. The inverse Fourier transform then gives the solution:

$$w(x) = \frac{1}{4\pi^2} \iint_{\mathbb{R}^2} \frac{12}{t^2} \frac{1}{\eta^4 + \alpha^4} \exp(-ix \cdot \xi) \, \mathrm{d}\xi$$

The product $x \cdot \xi$ is the usual inner product in $\mathbb{R}^n$.

We will calculate the integral above by transforming it into polar coordinates. We shall denote $\arg \xi = \psi$, $\arg x = \vartheta$ and $|x| = r$. Since w is radially symmetric we have $w(x) = w(r)$ and we can choose ϑ such that $x \cdot \xi = r\eta \sin \psi$. Then

$$w(r) = \frac{12}{2\pi t^2} \int_0^\infty \frac{\eta}{\eta^4 + \alpha^4} \frac{1}{2\pi} \int_{-\pi}^{\pi} \exp(-ir\eta \sin \vartheta) \, \mathrm{d}\vartheta \, \mathrm{d}\eta.$$

The inner integral can be simplified by noting that (see [LR99] for example)

$$J_0(z) = \frac{1}{2\pi} \int_{-\pi}^{\pi} \exp(-iz \sin \vartheta) \, \mathrm{d}\vartheta.$$

The function J_0 is a Bessel function and they are more thoroughly studied in Section 6.2.1. It remains to evaluate the one-dimensional integral

$$w(r) = \frac{12}{2\pi t^2} \int_0^\infty \frac{\eta J_0(r\eta)}{\eta^4 + \alpha^4} \, \mathrm{d}\eta$$

The integration tables of the Bessel functions, see [Łuk79], then give

$$w_0(r) = -\frac{6}{\pi\alpha^2} \operatorname{kei}(\alpha r).$$

We had a similar situation in Chapter 3 when one of the homogeneous solutions was also the solution of the non-homogeneous problem. In this case the term is $D \operatorname{kei}(\alpha r)$ and the coefficient D is

$$D = -\frac{6}{\pi\alpha^2}.$$

Hence,

$$w(r) = B\,\mathrm{ber}(\alpha r) + C\,\mathrm{bei}(\alpha r) - \frac{6}{\pi\alpha^2}\,\mathrm{kei}(\alpha r) + A$$

and

$$u(r) = -\frac{1+\nu}{R\alpha^2}D(\frac{r^3}{16}\log r - \frac{1}{\alpha r}) + \frac{F}{r} + [\text{smooth}]$$

Here smooth means terms that lie at least in H^1 . The energy condition $u \in \mathrm{H}^1$ then gives

$$F = -\frac{1+\nu}{R\alpha^3}D.$$

We will solve the remaining three constants A, B and C from the clamped boundary conditions

$$\begin{aligned}
w(L) &= A + B\,\mathrm{ber}(\alpha L) + C\,\mathrm{bei}(\alpha L) + D\,\mathrm{kei}(\alpha L) = 0 \\
w'(L) &= \alpha(B\,\mathrm{ber}'(\alpha L) + C\,\mathrm{bei}'(\alpha L) + D\,\mathrm{kei}'(\alpha L)) = 0 \\
u(L) &= -\frac{1+\nu}{R\alpha^2}(B\,\mathrm{bei}'(\alpha L) - C\,\mathrm{ber}'(\alpha L) - D\,\mathrm{ker}'(\alpha L)) - \frac{AL}{R} + \frac{F}{L} = 0
\end{aligned}$$

These constants are associated with the smooth terms of w so that they do not affect the behavior of w near origin. We will solve them just for completeness:

$$\begin{aligned}
A &= D(1+\nu)\frac{A_1}{A_2} \\
B &= D\frac{B_1}{B_2} \\
C &= D\frac{C_1}{C_2} \\
A_1 &= L\alpha((\mathrm{bei}')^2 + (\mathrm{ber}')^2)\,\mathrm{kei} \\
&\quad + \mathrm{bei}(\mathrm{ber}'(1 - L\alpha\,\mathrm{ker}') - L\alpha\,\mathrm{ber}'\,\mathrm{kei}') \\
&\quad + \mathrm{ber}(\mathrm{bei}'(-1 + L\alpha\,\mathrm{ker}') - L\alpha\,\mathrm{ber}'\,\mathrm{kei}') \\
A_2 &= L\alpha\left(LR\alpha^2\,\mathrm{ber}\,\mathrm{bei}' - (1+\nu)(\mathrm{bei}')^2 - \mathrm{ber}'(L\alpha^2\,\mathrm{bei} + (1+\nu)\,\mathrm{ber}')\right) \\
B_1 &= L\alpha\,\mathrm{kei}'(L\alpha^2\,\mathrm{bei} + (1+\nu)\,\mathrm{ber}') \\
&\quad - \mathrm{bei}'(L^2\alpha^3\,\mathrm{kei} + (1+\nu)(-1 + L\alpha\,\mathrm{ker}')) \\
B_2 &= L\alpha(L\alpha^2\,\mathrm{ber}\,\mathrm{bei}' - (1+\nu)(\mathrm{bei}')^2 - \mathrm{ber}'(L\alpha^2\,\mathrm{bei} + (1+\nu)\,\mathrm{ber}')) \\
C_1 &= L\alpha\,\mathrm{kei}'(-L\alpha^2\,\mathrm{ber} + (1+\nu)\,\mathrm{bei}') \\
&\quad + \mathrm{ber}'(L^2\alpha^3\,\mathrm{kei} + (1+\nu)(-1 + L\alpha\,\mathrm{ker}')) \\
C_2 &= B_2
\end{aligned}$$

where the Kelvin-functions are evaluated at

$$x = \alpha L = (12(1-\nu^2))^{1/4}\frac{L}{\sqrt{tR}}.$$

Typically $L < R$ but they are of the same order. Since we assumed that $\frac{t}{L}, \frac{t}{R} < 0.05$ (or similar) we have that

$$x > (12(1-1/4))^{1/4}\sqrt{\frac{L}{t}}\sqrt{\frac{L}{R}} > \sqrt{60}\frac{L}{R} \gg 1 \tag{5.19}$$

Hence, the coefficients A, B and C can be approximated with formulas (5.6). Doing this, we see that

$$\begin{aligned} A &\approx -\frac{D(1+\nu)}{L^2\alpha^3} = \mathcal{O}(t^{5/4}) \\ B &= \frac{(1+\nu)D\sqrt{2\pi x}}{L^2\alpha^3}\exp(-x/\sqrt{2})\left(\cos(\frac{\pi}{8}-\frac{x}{\sqrt{2}}) - \sin(\frac{\pi}{8}-\frac{x}{\sqrt{2}})\right) \\ &= \mathcal{O}(e^{-1/\sqrt{t}})) \\ C &= -\frac{(1+\nu)D\sqrt{2\pi x}}{L^2\alpha^3}\exp(-x/\sqrt{2})\left(\cos(\frac{\pi}{8}-\frac{x}{\sqrt{2}}) + \sin(\frac{\pi}{8}-\frac{x}{\sqrt{2}})\right) \\ &= \mathcal{O}(e^{-1/\sqrt{t}}) \end{aligned} \tag{5.20}$$

where $x = L\alpha$.

If we compare our result with that of the membrane theory, see Chapter 4, we see that the models differ considerably near the origin. However, when r is big enough, the two models start to resemble each other. We see this by approximation w when r is large:

$$\begin{aligned} w(r) &\approx e^{\alpha\frac{r}{\sqrt{2}}}\frac{1}{\sqrt{2\pi\alpha r}}\left(B\cos\left(\frac{\alpha r}{\sqrt{2}}-\frac{\pi}{8}\right) + C\sin\left(\frac{\alpha r}{\sqrt{2}}-\frac{\pi}{8}\right)\right) \\ &\quad + w_0 + D\exp(-\alpha\frac{r}{\sqrt{2}}) \end{aligned} \tag{5.21}$$

Using formulas (5.20) we see that

$$w(r) \approx f(r)\exp(\alpha(r-L)/\sqrt{2}) + D\exp(-\alpha r/\sqrt{2}) \tag{5.22}$$

where $f(r)$ consists of trigonometric and rational terms with respect to r. This means that w behaves like a constant near the boundary of the shell. Our membrane solution had a similar behaviour. Also, for the deformation u in Koiter model we get similarly

$$u(r) \approx g(r)\exp(\alpha(r-R)/\sqrt{2})$$

where g is similar to f in equation (5.22).

Returning to our solution near origin,

$$w = \frac{3}{2\pi}r^2\log r + [\text{smooth}] \tag{5.23}$$

where smooth means terms smoother than $r^3\log r$. For u we have

$$u = -\frac{(1+\nu)\alpha}{16R}r^3\log r + [\text{smooth}] \tag{5.24}$$

where smooth means terms smoother than $r^4\log r$. We see that the dominating term in w is the same approximate solution as in the equation (3.4) obtained when solving the Kirchhoff's model. This is what we anticipated and, indeed, near the origin the classical shell and plate solution do not notably differ. In Figure 5.1 we can see what u and w look like.

In Figure 5.2 we see that w seems to be smooth near the origin – as it should be.

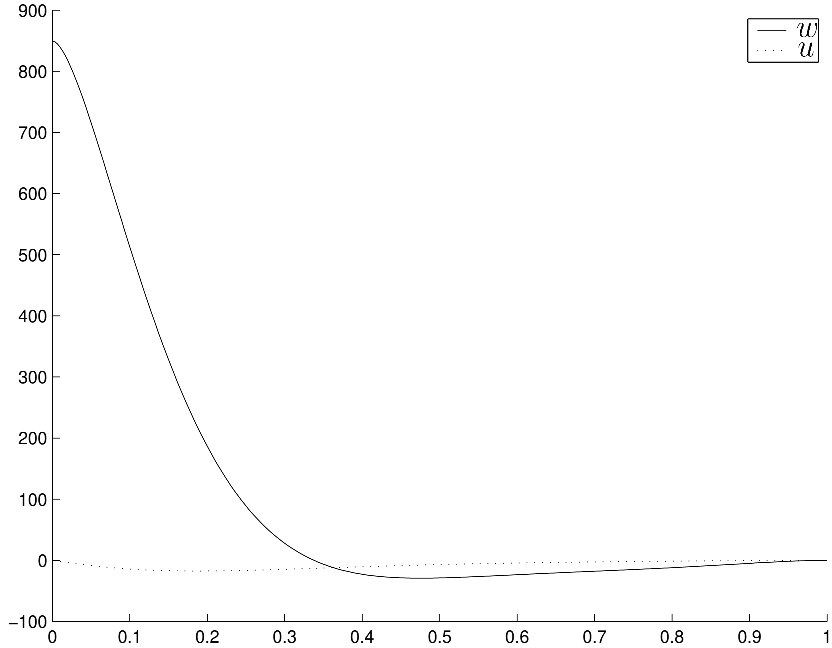

Figure 5.1: Deflections u and w (Koiter)

5.3 The Koiter layers

Let us study the relation of a and b defined in equations (2.19) and (2.20), respectively. If $r \approx L$ (or $r \gg \sqrt{t}$), then $w \approx 1, w' \approx 1/\sqrt{t}$ and $w'' \approx 1/tw$. We see then from equation (5.17) that $u \approx t$ and $u' \approx \sqrt{t}$. Then $a(\mathbf{u}, \mathbf{u}) \approx 1$ whereas $b(\mathbf{u}, \mathbf{u}) \approx 1/t^2$. Hence,

$$a(\mathbf{u}, \mathbf{u}) \leq Ct^2 b(\mathbf{u}, \mathbf{u})$$

and the problem is bending-dominated such that it locks if p in equation (2.24) is too small. If we have $r > \sqrt{t}$ but we are near the layer $\sqrt{t}$ we still have locking but our error is

$$K \approx 1/\sqrt{t}$$

so that it is more bearable than when r is larger. Since p has already been increased to avoid locking in scale $r \approx 1$ we only need to refine our mesh in interval $[0, s]$ where s is our dominating length scale. The standard choice – to be on the safe side – is usually $[0, 2s]$.

If $r \approx \sqrt{t}$ we have $w', w'', u' \approx 1$ so that $a(\mathbf{u}, \mathbf{u}) \approx b(\mathbf{u}, \mathbf{u})$ and we cannot be sure about locking. By the calculations above we may assume locking but it is not as serious for small r.

Let us next study the layers near origin. The mode $r \approx 1$ is the solution of the membrane problem:

$$w \approx \frac{R^2}{1 - \nu^2}\delta.$$

When $r \approx t$,

$$\alpha r \approx (12(1 - \nu^2)/R^2)^{1/4}\sqrt{t} \ll 1.$$

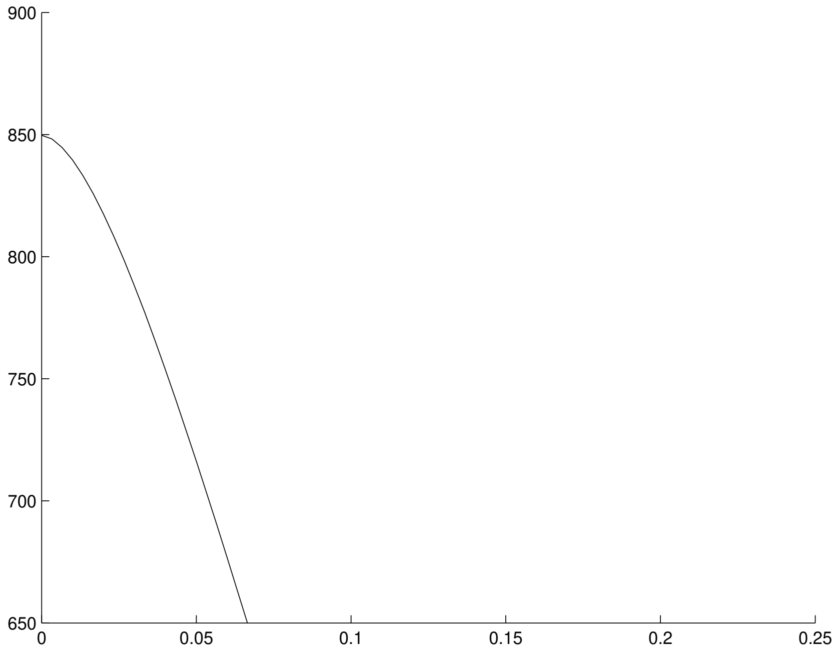

Figure 5.2: Deflection w near the origin (Koiter)

Then the solution is given by equation (5.23) so no exponential solution is present and thus we do not have the mode $n = 1$ as suspected in Section 2.5.

When $n = 2$,

$$\alpha r \approx (12(1-\nu^2)/R^2) \gg 10$$

and the solution is given in equation (5.22) which has the term

$$e^{-r/\sqrt{t}}.$$

Hence, we have the mode $n = 2$ as suspected.

When we are near the boundary, equation (5.22) applies again and we have the modes $n = 2$ and $r \approx 1$. No other modes are present.

Hence, the refinement should be done to the distance $2\sqrt{t}$ from the origin and, if necessary, the same distance from the boundary.

Chapter 6

Circular shell Naghdi

In this Chapter we will solve the Naghdi model for thin shells. The model differs from the Koiter's model studied in Chapter 5 by including the shearing strains to the model. This also affects the energy conditions of the problem, the solution will be not as smooth as Koiter's solution. The counterpart of Naghdi model in plates is Reissner-Mindlin model, studied in Section 3.3.

First we will derive the Euler equations for the problem. Then we will state a few facts about Bessel functions, since the solution will essentially consist of them. Finally, we will solve the Naghdi problem and study its behavior near the origin and boundary.

6.1 The Naghdi shell equations

The energy functional of the Naghdi model is

$$\begin{aligned}\mathcal{F}(\mathbf{u}) &= \frac{1}{2}\int_\omega \nu(\beta_{11}+\beta_{22})^2 + (1-\nu)(\beta_{11}^2 + 2\beta_{12}^2 + \beta_{22}^2)\,d\omega \\ &+ \frac{k}{2}\int_\omega (\rho_1^2 + \rho_2^2)\,d\omega \\ &+ \frac{t^2}{24}\int_\omega \nu(\kappa_{11}+\kappa_{22})^2 + (1-\nu)(\kappa_{11}^2 + 2\kappa_{12}^2 + \kappa_{22}^2)\,d\omega, \\ 2k &= \gamma(1-\nu)\end{aligned} \tag{6.1}$$

where tensors β_{11}, β_{12}, β_{22}, κ_{11}, κ_{12}, κ_{22}, ρ_1 and ρ_2 are in this spherical case defined by

$$\begin{cases} \beta_{11} = u' + w/R \\ \beta_{12} = 0 \\ \beta_{22} = u/r + w/R \\ \kappa_{11} = \theta' \\ \kappa_{12} = 0 \\ \kappa_{22} = \theta/r \\ \rho_1 = -w' + u/R + \theta \\ \rho_2 = 0 \end{cases} . \tag{6.2}$$

By using the standard Method of Variations we get the Euler equations for the Naghdi model:

$$\begin{aligned} \delta u &: \frac{u}{r} - u' - ru'' + \frac{k}{R^2}ru - \frac{k+1+\nu}{R}rw' + \frac{k}{R}r\theta = 0 \\ \delta w &: \frac{k+1+\nu}{R}(ru' + u) + k(r\theta' + \theta) + \frac{2(1+\nu)}{R^2}rw - k(rw'' + w') = \delta r \\ \delta\theta &: kr(\theta + \frac{u}{R} - w') + \frac{t^2}{12}(\frac{\theta}{r} - \theta' - \theta'' r) = 0 \end{aligned} \tag{6.3}$$

The boundary conditions are now $u(L) = w(L) = \theta(L) = 0$. We see that this problem is very much like the Reissner-Mindlin's plate problem in Section 3.3. We shall use the ideas used in that Section to solve this more difficult problem. In fact, we shall see that the solutions for the both problems shall be very similar.

6.2 Solving the Naghdi equations

6.2.1 Bessel functions

We will shortly state some facts on Bessel functions in this Section. The Bessel functions are the solutions for the Bessel differential equation

$$z^2u''(z) + zu'(z) + (p^2z^2 - \alpha^2)u(z) = 0, z \in \mathbb{C}\,(\text{ or } \mathbb{R})$$

where p and α are some real or complex constants. The solutions are denoted by $J_\alpha(pz)$ and $Y_\alpha(pz)$. Function J_α is smooth near origin whereas Y_α is singular. If $\alpha = 0$, we have the series representation

$$\begin{aligned} J_0(z) &= 1 - z^2/4 + \mathcal{O}(z^4) \\ Y_0(z) &= \frac{2}{\pi}\left(\ln(\frac{z}{2}) + \gamma\right)J_0(z) + \frac{2}{\pi}\frac{z^2}{4} + \mathcal{O}(z^4) \\ &= \frac{2}{\pi}\left(\left(1 - \frac{z^2}{4}\right)\ln(\frac{z}{2}) + \gamma + \frac{z^2}{4}\right) + \mathcal{O}(z^4) \end{aligned} \tag{6.4}$$

and if $\alpha = 1$,

$$\begin{aligned} J_1(z) &= \frac{z}{2} + \mathcal{O}(z^3) \\ Y_1(z) &= \frac{2}{\pi}\left(-\frac{1}{2} + \gamma + \ln(\frac{z}{2})\right) J_1(z) - \frac{z}{2\pi} + \mathcal{O}(z^3) \\ &= -\frac{2}{\pi z} - \frac{1}{\pi}\left(\frac{1}{2} - \gamma + \ln(\frac{2}{z})\right) + \mathcal{O}(z^3) \end{aligned} \tag{6.5}$$

If $z \to \infty$ we get, for $n \in \mathbb{N}$,

$$\begin{aligned} J_n(z) &= \sqrt{\frac{2}{\pi z}}\left(\cos(z - \frac{\pi}{4} - \frac{n\pi}{2}) + \mathcal{O}(\frac{1}{z})\right) \\ Y_n(z) &= \sqrt{\frac{2}{\pi z}}\left(\sin(z - \frac{\pi}{4} - \frac{n\pi}{2}) + \mathcal{O}(\frac{1}{z})\right). \end{aligned} \tag{6.6}$$

We have also that $J_0'(z) = -J_1(z)$ and $Y_0'(z) = -Y_1(z)$. The complex conjugates of any Bessel function satisfy

$$\bar{f}(z) = f(\bar{z}). \tag{6.7}$$

Here $\bar{z}$ denotes the complex conjugate of z. For more information, see [LR99] or [MA65].

6.2.2 The Nagdhi solution

Let us now solve the Euler equations of the Naghdi model. First we can see that the vectors

$$\mathbf{u}_1 = (u, \theta, w) = (r, -\frac{r}{R}, -R)$$

and

$$\mathbf{u}_2 = (\frac{1}{r}, -\frac{1}{rR}, 0)$$

solve the equations. They correspond to the layer $r \approx 1$ since they do not depend on t. Now we need more solutions. We continue by making the ansatz $u = aw'$, $\theta = bw'$, where a and b are unknown constants. This ansatz is motivated by the similarity between the Koiter and Naghdi models and the symmetry of the differential equations. Substituting this ansatz into the equations we get from δw

$$rw'' + w' + p_1^2 wr = 0, \tag{6.8}$$

where

$$p_1^2 = \frac{2(1+\nu)}{(a\frac{k+1+\nu}{R} + kb - k)R^2}. \tag{6.9}$$

Equation (6.8) is a Bessel differential equations for w. It can be solved with the Bessel functions

$$w = C_0 J_0(p_1 r) + D_0 Y_0(p_1 r).$$

Since $u = aw'$ and $\theta = bw'$ and $J_0' = -J_1$, $Y_0' = -Y_1$, we see that u and θ must be Bessel functions

$$\begin{aligned} u &= -ap_1C_0J_1(p_1r) - ap_1D_0Y_1(p_1r) \\ \theta &= -bp_1C_0J_1(p_1r) - bp_1D_0Y_1(p_1r). \end{aligned}$$

We can write the solutions as vectors

$$\mathbf{u}_3 = (-ap_1J_1(p_1r), -bp_1J_1(p_1r), J_0(p_1r))$$

and

$$\mathbf{u}_4 = (-ap_1Y_1(p_1r), -bp_1Y_1(p_1r), Y_0(p_1r)).$$

assuming we find suitable a, b and p_1. The Euler equations for δu and $\delta\theta$ can now be written as Bessel's equations

$$\begin{aligned} \delta u &: r^2u'' + ru' + (p_2^2 - 1)u = 0 \\ \delta\theta &: r^2\theta'' + r\theta' + (p_3^2 - 1)\theta = 0. \end{aligned}$$

We see that the equations are satisfied if the constants a and b satisfy the conditions

$$p_1^2 = p_2^2 = p_3^2. \tag{6.10}$$

These conditions correspond to two second order polynomial equations for a and b, the solutions of which can be seen to be complex. The solutions are

$$\begin{aligned} a &= \frac{a_1}{a_2} \\ a_1 &= -Rt(6R^2tk(\nu^2 - 1 + 4k) + t^3(-1 + \nu^2 + 2k + 2\nu k + 2k^2) \\ &\quad + (t^2 + 6R^2)\sqrt{s}) \\ a_2 &= 2(-t^2 + 6R^2(-1 + \nu))k(12R^2k + t^2(1 + \nu + k)) \\ b &= \frac{b_1}{b_2} \\ b_1 &= 3R^2(24R^2(\nu - 1)k^2 + t^2(\nu - 1)(\nu^2 - 1 + 3k + 3\nu k + 2k^2) \\ &\quad + t(-1 + \nu + k)\sqrt{s}) \\ b_2 &= (-t^2 + 6R^2(-1 + \nu))k(12R^2k + t^2(1 + \nu + k)) \\ p &= p_1 = \sqrt{q} \\ q &= 4k(t^2 - 6R^2(-1 + \nu))(1 + \nu)/(R^2t(t(1 + \nu)(-1 + \nu + 2k) + \sqrt{s})) \\ s &= (-1 + \nu^2)(48R^2k^2 + t^2(-1 + \nu^2 + 4k + 4\nu k + 4k^2)) \end{aligned} \tag{6.11}$$

Since $t \ll 1$, we can approximate

$$\begin{aligned} a &= \hat{a}ti + \mathcal{O}(t^2), \text{ where } \hat{a} = -\frac{\sqrt{1-\nu^2}}{2\sqrt{3}(\nu - 1)} \in \mathbb{R} \\ b &= 1 + \hat{b}ti + \mathcal{O}(t^2), \text{ where } \hat{b} = \frac{\sqrt{1-\nu^2}(\nu + k + 1)}{2\sqrt{3}R(\nu - 1)} \in \mathbb{R} \\ p^2 &= \frac{\hat{p}}{t}i + \mathcal{O}(1), \text{ where } \hat{p} = -\frac{2\sqrt{3(1-\nu^2)}}{R} \in \mathbb{R}. \end{aligned} \tag{6.12}$$

We see from equation (6.9) that if we replace a with $\bar{a}$ and b with $\bar{b}$ we get $\bar{p}$ (instead of p). We get then two solutions for our equations (6.10): (a, b, p) and $(\bar{a}, \bar{b}, \bar{p})$. Then in addition to $\mathbf{u}_3$ and $\mathbf{u}_4$ also vectors

$$\mathbf{u}_5 = (-a\bar{p}_1 J_1(\bar{p}_1 r), -\bar{b}\bar{p}_1 J_1(\bar{p}_1 r), J_0(\bar{p}_1 r))$$

and

$$\mathbf{u}_6 = (-a\bar{p}_1 Y_1(\bar{p}_1 r), -\bar{b}\bar{p}_1 Y_1(\bar{p}_1 r), Y_0(\bar{p}_1 r))$$

satisfy the homogeneous equation. Since our problem was uniquely solvable and it was of sixth degree, the six vectors generate the solution for the homogeneous equation and it can be written in the scalar form as

$$\begin{aligned}
w &= -AR + CJ_0(pr) + DJ_0(\bar{p}r) + EY_0(pr) + FY_0(\bar{p}r) \\
u &= Ar + \frac{B}{r} - (CapJ_1(pr) + D\bar{a}\bar{p}J_1(\bar{p}r) + EapY_1(pr) + F\bar{a}\bar{p}Y_1(\bar{p}r)) \\
\theta &= -\frac{1}{R}(Ar + \frac{B}{r}) \\
&\quad - \left(CbpJ_1(pr) + D\bar{b}\bar{p}J_1(\bar{p}r) + EbpY_1(pr) + F\bar{b}\bar{p}Y_1(\bar{p}r)\right).
\end{aligned} \tag{6.13}$$

Since the solution of the real, linear system of differential equations (6.3) should be real we shall try to write the solutions in a real form. With the help of equation (6.7) we can then make the transformation

$$Af(z) + Bf(\bar{z}) = Af(z) + B\bar{f}(z) = \hat{A}\,\mathrm{Re}\, f(z) + \hat{B}\,\mathrm{Im}\, f(z),$$

where Re denotes the real part and Im denotes the imaginary part. We have the following transformation equations

$$\begin{aligned}
\hat{A} &= A + B \\
\hat{B} &= i(A - B).
\end{aligned} \tag{6.14}$$

Hence we get the following solution for the homogeneous Euler equations in the "real form":

$$\begin{aligned}
w &= -AR + C\,\mathrm{Re}\, J_0(pr) + D\,\mathrm{Im}\, J_0(pr) + E\,\mathrm{Re}\, Y_0(pr) + F\,\mathrm{Im}\, Y_0(pr) \\
u &= Ar + \frac{B}{r} - C\,\mathrm{Re}(apJ_1(pr)) - D\,\mathrm{Im}(apJ_1(pr)) \\
&- E\,\mathrm{Re}(apY_1(pr)) - F\,\mathrm{Im}(apY_1(pr)) \\
\theta &= -\frac{1}{R}(Ar + \frac{B}{r}) - C\,\mathrm{Re}(bpJ_1(pr)) - D\,\mathrm{Im}(bpJ_1(pr)) \\
&- E\,\mathrm{Re}(bpY_1(pr)) - F\,\mathrm{Im}(bpY_1(pr)).
\end{aligned} \tag{6.15}$$

A particular solution for the whole system in the distributive sense can be determined in the same way as in Section 3.3: We write $w = w_0 + w_1$, where $w_0 \in \mathrm{H}^2$, i.e., it corresponds to the Koiter model of the problem, and w_1 will be the singular part of the solution. We have $u = u_0 \in \mathrm{H}^1$ and $\theta = \theta_0 \in \mathrm{H}^1$. The only singularity – and the term that separates the Naghdi's solution from the Koiter's solution – comes from w_1. This is what happened to the plate as well. We will write

$$t^2 q = k(\theta + \frac{u}{R} - w') \tag{6.16}$$

so that when $u = u_0$, $\theta = \theta_0$ and $w = w_0 + w_1$, $q = q_0 + q_1$. Let us denote the linear elastic operator by

$$\mathcal{G}(\theta) = -\theta'' - \frac{\theta'}{r} + \frac{\theta}{r^2}.$$

It is similar to that in the Reissner-Mindlin's Plate equation (3.18).

We get the following equations for w_0, w_1, u and θ:

$$\begin{aligned}
\frac{1+\nu}{R}\left(u_0' + \frac{u_0}{r}\right) + \frac{2}{R^2}(1+\nu)w_0 + t^2\nabla\cdot(q_0\,\mathbf{e}_3) &= 0 & (6.17)\\
t^2\nabla\cdot(q_1\,\mathbf{e}_3) + \frac{2}{R^2}(1+\nu)w_1 &= t^2\delta & (6.18)\\
12q_0 + \mathcal{G}\theta &= -12q_1 & (6.19)\\
\left(\frac{u_0}{r^2} - \frac{u_0'}{r} - u_0'' + \frac{1}{Rt^2}q_0\right)\,\mathbf{e}_3 + \frac{1+\nu}{R}\nabla w_0 & & \\
-\frac{1}{R}\left(\frac{k}{t^2} - 1 - \nu\right)\nabla w_1 &= 0. & (6.20)
\end{aligned}$$

We can differentiate the equation (6.16) so that we can substitute $\nabla\cdot(q\,\mathbf{e}_3)$ to the equations above. Then from equation (6.18) we get the distributive equation

$$-\triangle w_1 + \beta^2 w_1 = \frac{t^2}{k}\delta, \tag{6.21}$$

where

$$\beta^2 = \frac{2(1+\nu)}{R^2t^2}.$$

Then $w_1 \in \mathrm{H}^0 = L^2$ by Theorem 2.4. The other functions can be seen to satisfy the classical energy conditions as we anticipated. We can now solve the equation (6.21) by Fourier transformation. We use similar technique to the one used in Section 5.2. For the Fourier transformation $\hat{w}(\xi)$ of $w(x)$ we have

$$\hat{w}(\xi) = \frac{t^2}{k(\beta^2 - \eta^2)}$$

where $\eta = |\xi|$. We will also denote $\arg\xi = \psi, |x| = r$ and $\arg x = \varphi$. The inverse transformation yields

$$w(x) = \frac{1}{4\pi^2}\iint_{\mathbb{R}^2} \frac{t^2}{k(\beta^2-\eta^2)} e^{-ix\cdot\xi}\,\mathrm{d}\eta.$$

Since the solution $w(x) = w(r)$ is radially symmetric we can choose φ such that $x\cdot\xi = r\eta\sin\psi$. Using the integral tables of for example [Łuk79] we finally get

$$\begin{aligned} w(r) &= \frac{1}{2\pi}\int_0^\infty \frac{t^2}{k}\frac{\eta\,\mathrm{d}\eta}{\beta^2-\eta^2}\frac{1}{2\pi}\int_{-\pi}^{\pi}\exp(-ir\eta\sin\psi)\,\mathrm{d}\psi \\ &= \frac{t^2}{2\pi k}\int_0^\infty \frac{\eta}{\beta^2-\eta^2}J_0(r\eta)\,\mathrm{d}\eta \\ &= -\frac{t^2}{4k}Y_0(\beta r) = w_1(r). \end{aligned} \tag{6.22}$$

By equation (6.5), near the origin

$$Y_0(\beta r) = \ln r + [\text{smooth}]$$

so that the solution does not depend on the parameter β near origin. Here [smooth] means terms that lie in H^2 at least. Hence, the particular solution for the nonhomogeneous system is also one of the homogeneous solutions. This is what we got in the earlier models too, in Chapters 3 and 5. The dominating terms of homogeneous solution w in equation (6.13) are

$$\begin{aligned} &EY_0(pr) + FY_0(\bar{p}r) \\ &= \frac{2}{\pi}\ln r\left(E\left(1-\frac{p^2r^2}{4}\right)+F\left(1-\frac{\bar{p}^2r^2}{4}\right)\right)+[\text{smooth}]. \end{aligned} \tag{6.23}$$

Here smooth means terms that lie in H^3, at least. On the other hand, the singular solution of the nonhomogeneous equations is

$$w_1 = -\frac{t^2}{4k}Y_0(\beta r) = -\frac{2t^2}{4k\pi}\ln r + [\text{smooth}]$$

and we get an equation for the coefficients E and F:

$$E + F = -\frac{t^2}{4k}. \tag{6.24}$$

Now $w_0 \in \mathrm{H}^2$ since it consists of the smooth part of w. Let us study the remaining deflections u_0 and θ_0 as they should lie in H^1.

$$\begin{aligned} \theta_0 &= -\frac{B}{Rr} - (bY_1(pr)pE + \bar{b}Y_1(\bar{p}r)\bar{p}F) + [\text{smooth}] \\ &= -\frac{1}{r}\left(\frac{B}{R} - \frac{2}{\pi}Eb - \frac{2}{\pi}F\bar{b}\right) + [\text{smooth}] \end{aligned} \tag{6.25}$$

and we get

$$\frac{B}{R} - \frac{2}{\pi}Eb - \frac{2}{\pi}F\bar{b} = 0. \tag{6.26}$$

In a similar way we get for $u_0 \in \mathrm{H}^1$ the condition

$$B + \frac{2}{\pi}Ea + \frac{2}{\pi}F\bar{a} = 0. \tag{6.27}$$

We have gained three equations (6.24), (6.26) and (6.27) for the coefficients B, E and F whose solution is

$$
\begin{aligned}
B &= \frac{t^2 R(a\bar{b} - b\bar{a})}{2\pi k(a - \bar{a} + R(b - \bar{b}))} \approx -\frac{\hat{a} R t^2}{2\pi k(\hat{a} + \hat{b} R)} && (6.28)\\
E &= \frac{(\bar{a} + R\bar{b})t^2}{4k(a - \bar{a} + R(b - \bar{b}))} \approx -\frac{(\hat{a} + R\hat{b})t^2 + Rti}{8k(\hat{a} + \hat{b}R)} && (6.29)\\
F &= -\frac{(a + Rb)t^2}{4k(a - \bar{a} + R(b - \bar{b}))} \approx -\frac{(\hat{a} + R\hat{b})t^2 - Rti}{8k(\hat{a} + \hat{b}R)}. && (6.30)
\end{aligned}
$$

Finally, the coefficients of the smooth terms A, C and D can be solved from the clamped boundary conditions

$$
\begin{aligned}
w(L) &= -AR + CJ_0(pL) + DJ_0(\bar{p}L) + EY_0(pL) + FY_0(\bar{p}L) = 0\\
u(L) &= AL + B/L\\
&\quad - (apCJ_1(pL) + \bar{a}\bar{p}DJ_1(\bar{p}L) + apEY_1(pL) + \bar{a}\bar{p}FY_1(\bar{p}L)) = 0\\
\theta(L) &= -\frac{AL}{R} - \frac{B}{LR}\\
&\quad - (bpCJ_1(pL) + \bar{b}\bar{p}DJ_1(\bar{p}L) + bpEY_1(pL) + \bar{b}\bar{p}FY_1(\bar{p}L)) = 0.
\end{aligned}
\tag{6.31}
$$

The solution is

$$
\begin{aligned}
A =& \frac{A_1}{A_2}\\
A_1 =& (b\bar{a} - a\bar{b})R(J_1(\bar{J}_1\bar{Y}_0\bar{p}L\pi - \bar{J}_0(2 + \bar{Y}_1\bar{p}L\pi))(a + bR)p\\
&+ \bar{a}\bar{J}_1\bar{p}(-J_1 L\pi Y_0 p + J_0(2 + L\pi Y_1 p))\\
&+ \bar{b}\bar{J}_1\bar{p}R(-J_1 L\pi Y_0 p + J_0(2 + L\pi Y_1 p)))\\
A_2 =& 4kL\pi(a - \bar{a} + R(b - \bar{b}))\\
&(\bar{J}_0 J_1 L(a + bR)p + \bar{b}\bar{J}_1\bar{p}R(-J_0 L + aJ_1 Rp) - \bar{a}\bar{J}_1\bar{p}(J_0 L + bJ_1 R^2 p))\\
C =& (\bar{a} + \bar{b}R)\frac{C_1}{C_2}\\
C_1 =& \bar{J}_1\bar{p}L^2\pi(\bar{a} + \bar{b}R)Y_0\\
&+ bR(\bar{J}_0 L^2\pi(\bar{Y}_1\bar{p} - Y_1 p) + \bar{J}_1\bar{p}(-\bar{Y}_0 L^2\pi + \bar{a}R(2 + L\pi Y_1 p)))\\
&- a(\bar{J}_0 L^2\pi(-\bar{Y}_1\bar{p} + Y_1 p) + \bar{J}_1\bar{p}(\bar{Y}_0 L^2\pi + \bar{b}R^2(2 + L\pi Y_1 p)))\\
C_2 =& A_2\\
D =& \bar{C}.
\end{aligned}
\tag{6.32}
$$

Here the Bessel functions are evaluated at $z = pL$. We also assumed in equation (2.1) that $\frac{t}{R} \leq 0.05$. Hence,

$$
\begin{aligned}
|pL| &\approx \sqrt{\hat{p}/2t}L\\
&= \sqrt[4]{6(1 - \nu^2)R^2/t^2}L\\
&> \sqrt[4]{3}\sqrt{R/t}L\\
&\gg L/0.05\sqrt[4]{3} \gg 1.
\end{aligned}
\tag{6.33}
$$

Then the we can approximate the Bessel functions by equations (6.6). Let us denote $x = \operatorname{Re} z = |pL|/\sqrt{2}$ and note that $z = x(1-i)$. Then

$$\begin{aligned}\cos z &= \cos x \cosh x + i \sin x \sinh x\\ \sin z &= \sin x \cosh x - i \cos x \sinh x\end{aligned}$$

and the Bessel functions will be

$$\approx \frac{1}{\sqrt{\pi L p}}(e^{xr} f(r) + e^{-xr} g(r)).$$

Here f and g consist of terms whose absolute values consist of trigonometric functions and the coefficient $1/\sqrt{z}$. The coefficient is not essential in these calculations. Hence, when we solve the A, C and D from the equations (6.31) we essentially get solutions for which the e^{xr} terms must vanish. What remains, are the terms e^{-xr}. Hence, when t is small and $r \approx L$,

$$w \approx \exp(-xr) = \exp(-\frac{\hat{p}L}{\sqrt{2t}} r) h(r), \tag{6.34}$$

where $h(r)$ consists of terms that are essentially trigonometric. Note that A will be approximately

$$A \approx e^x t^{-1/4}.$$

When $r \ll 1$ the smooth terms can be neglected. Let us study the behavior of the shell near the origin. Hence, in the real form

$$\begin{aligned}
w &= (E+F)\operatorname{Re}(Y_0(pr)) + i(E-F)\operatorname{Im}(Y_0(pr)) + [\text{smooth}]\\
&= -\frac{t^2}{4k}\operatorname{Re}(Y_0(pr)) + [\text{smooth}]\\
&= -\frac{t^2}{2\pi k}\ln r + \frac{3}{2\pi} r^2 \ln r + [\text{smooth}]\\
u &= B/r - (E+F)\operatorname{Re}(apY_1(pr)) - i(E-F)\operatorname{Im}(apY_1(pr)) + [\text{smooth}]\\
&= \frac{t^2}{4\pi k}\hat{a}\hat{p} r \ln r + [\text{smooth}]\\
&= \frac{t^2(1+\nu)}{4\pi k R} r \ln r + [\text{smooth}]\\
\theta &= -B/rR - (E+F)\operatorname{Re}(bpY_1(pr)) - i(E-F)\operatorname{Im}(bpY_1(pr)) + [\text{smooth}]\\
&= \frac{t^2}{4\pi k}\hat{p}(\hat{b} + \frac{2R\sqrt{3}k}{t^2\sqrt{1-\nu^2}}) r \ln r + [\text{smooth}]
\end{aligned}$$

and we see that this solution resembles the Reissner-Mindlin model for plates. We also see that the difference between Koiter and Naghdi is in essence the term

$$w_1 \approx \frac{t^2}{2\pi k}\ln r.$$

When t is small this term becomes negligible when compared to the smoother term

$$w_0 \approx \frac{3}{2\pi} r^2 \ln r$$

of the Naghdi-solutions. This term is similar to the Koiter's solution, see equations (5.23). In Figure 6.1 we see both w and θ. The deflection u is so small compared to w and θ (in absolute value) that it seems to be on the x-axes.

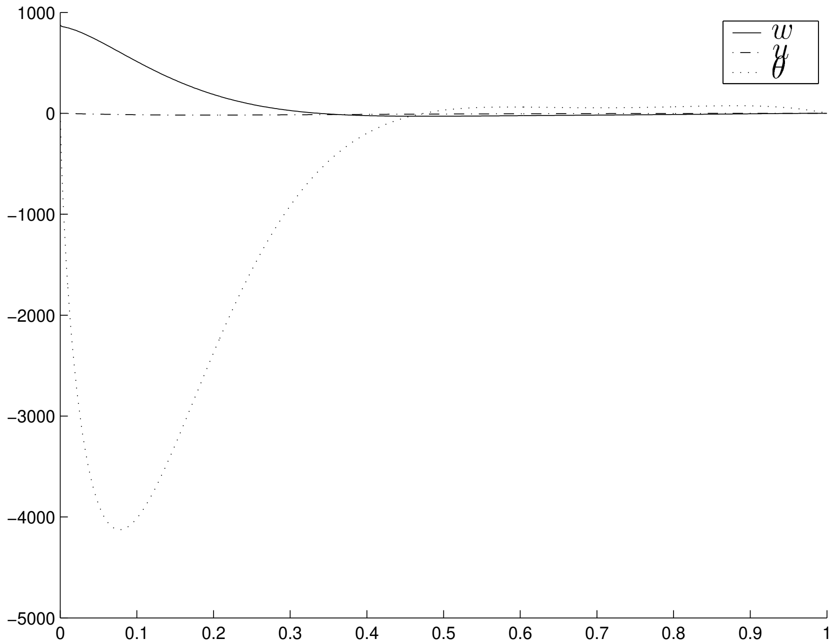

Figure 6.1: Naghdi's u, θ and w.

In Figure 6.2 we see that there is a small spike near the origin – this is the effect of the logarithmic term in the solution.

6.3 The Naghdi layers

We will first note that Naghdi's model locks. If $r \approx L$ and let $w \approx 1$ and $w' \approx 1/\sqrt{t}$ (we can always scale w this way). Then $u, u' \approx t\frac{1}{\sqrt{t}} = \sqrt{t}$ and $\theta \approx 1/\sqrt{t}$ and $\theta' \approx 1/t$. Then the membrane energy $a(\mathbf{u}, \mathbf{u}) \approx 1$ and the bending energy $b(\mathbf{u}, \mathbf{u}) \approx 1/t^2$. Hence,

$$a(\mathbf{u}, \mathbf{u}) \leq t^2 b(\mathbf{u}, \mathbf{u})$$

and Naghdi is bending dominated. If $r > \sqrt{t}$ but we are near $\sqrt{t}$ we get still locking but the error is not as bad as for large r. The same deduction was done in Section 5.3.

If $r \approx \sqrt{t}$, we have $w', \theta, \theta' \approx w$ and $u, u' \approx tw$. Then $a(\mathbf{u}, \mathbf{u}) \approx w^2$ and $b(\mathbf{u}, \mathbf{u}) \approx w^2$ and the system is membrane dominated. In that case we may have locking and we see it only by testing the solver. However, we could assume locking since when $r > \sqrt{t}$ we had locking. If we have locking we must first increase p. Otherwise, it is enough to refine the mesh.

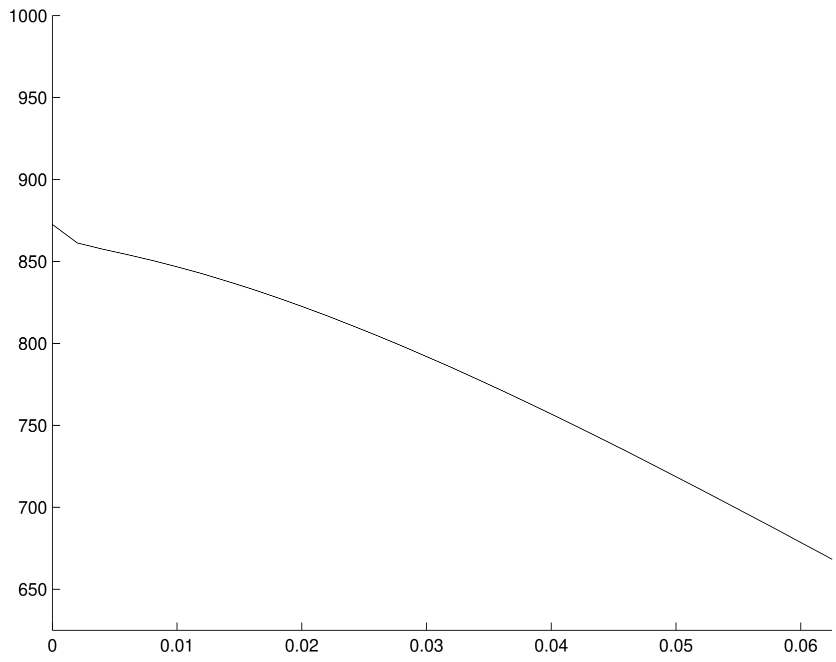

Figure 6.2: Naghdi's w near the origin.

Let us look at the layers of the Naghdi model. Layers were shortly described in Section 2.5. First, the layer for $r \approx 1$ is

$$w = -AR.$$

When $n = 1$ we have

$$\begin{aligned} |pr| &\approx \sqrt[4]{6(1-\nu^2)R^2}\sqrt{2t} \\ &< \sqrt[4]{6}\sqrt{tR} < 1 \end{aligned} \tag{6.35}$$

if t is small. Hence, the solution is given by equation (6.2.2) and there is no exponential decay of order t.

When $n = 2$ we get

$$|pr| \approx \sqrt[4]{12(1-\nu^2)R^2} > \sqrt{3R} \gg 1 \tag{6.36}$$

and the solution is given by equation (6.34) and we have the mode $n = 2$.

Near the boundary, $r \approx L$ and equation (6.33) applies for pr. Hence the solution is given by (6.34) and we only have the mode $n = 2$.

Chapter 7

Numerical experiment

In this Chapter we will solve both the Koiter (Chapter 5) and Naghdi (Chapter 6) models with Finite Element Method (FEM). We will choose the appropriate element spaces as well as the mesh for the problem. We will also study locking which was defined in Section 2.5.

7.1 Naghdi

In this Section we shall construct the matrix $\mathbf{A}$ and the vector $\mathbf{b}$ for the linear problem defined in previous Section. First, the matrices $\mathbf{S}_\beta$ and $\mathbf{D}_\beta$ corresponding to the membrane strain are

$$\mathbf{S}_\beta = \begin{pmatrix} \frac{d}{dr} & 0 & \frac{1}{R} \\ \frac{1}{r} & 0 & \frac{1}{R} \end{pmatrix} \; \mathbf{D}_\beta = \begin{pmatrix} 1 & \nu \\ \nu & 1 \end{pmatrix}. \tag{7.1}$$

Next, the matrices $\mathbf{S}_\kappa$ and $\mathbf{D}_\kappa$ corresponding to the bending strain are

$$\mathbf{S}_\kappa = \begin{pmatrix} 0 & \frac{d}{dr} & 0 \\ 0 & \frac{1}{r} & 0 \end{pmatrix} \; \mathbf{D}_\kappa = \frac{t^2}{12} \begin{pmatrix} 1 & \nu \\ \nu & 1 \end{pmatrix} \tag{7.2}$$

, and last, the matrices $\mathbf{S}_\rho$ and $\mathbf{D}_\rho$ corresponding to the shear tensor are

$$\mathbf{S}_\rho = \begin{pmatrix} \frac{1}{R} & 1 & -\frac{d}{dr} \\ 0 & 0 & 0 \end{pmatrix} \; \mathbf{D}_\kappa = kI = k \begin{pmatrix} 1 & 0 \\ 0 & 1 \end{pmatrix}. \tag{7.3}$$

As noted in Section 6.2.2, $\mathbf{u} \in \mathrm{H}_0^1 \times \mathrm{H}_0^1 \times \mathrm{H}_0^2$. This means that we should have polynomials of first degree for u and θ and polynomials of third degree for w. However, since $\theta \approx w'$, we need to add second order polynomials to θ. We will also add them to u as well in order to simplify the code.

The support condition mentioned in equation (2.34) can be simply stated as

$$\varphi_i^h(r_j) = 0, i \neq j.$$

We can add one more condition to get unique first degree elements. Let it be

$$\varphi_i^h(r_i) = 1.$$

Then we get that the first degree polynomials are

$$\varphi_i = \begin{cases} (r - r_{k-1})/h_k, & x_{k-1} \le r \le x_k \\ (r_{k+1} - r)/h_{k+1}, & x_k \le r \le x_{k+1} \\ 0, & \text{otherwise.} \end{cases} \tag{7.4}$$

We will reserve φ for the linear elements and denote elements of higher degree with different notation. The second degree polynomial is a "bubble" defined by the conditions

$$\phi_i(x_j) = 0, \, \forall j.$$

We can choose the third condition to be

$$\phi_i((x_{i-1} + x_i)/2) = 1, \, \forall i.$$

Then the second degree element is uniquely defined to be

$$\phi_i = \begin{cases} (r - r_{j-1})(r_j - r)/h_j^2, & r_{j-1} \le r \le r_j \\ 0, & \text{otherwise} \end{cases}$$

Finally, there are two third degree functions for each segment $[r_{j-1}, r_{j+1}]$. Let us denote them by ψ^a and ψ^b. They both will satisfy

$$\psi_j(r_{j-1}) = \psi_j(r_{j+1}) = 0.$$

In addition we demand that

$$(\psi_j^a)'(r_j) = 0, \, \psi_j^a(r_j) = 1$$

and

$$(\psi_j^b)'(r_j) = 1, \, \psi_j^b(r_j) = 0.$$

Then ψ^a and ψ^b are linearly independent. Hence, the cubic elements will be

$$\psi_j^a(r) = \begin{cases} (r - r_{j-1})^2 \left(2(r_j - r) + h_j\right)/h_j^3, & r_{j-1} \le r \le r_j \\ (r_{j+1} - r)^2 \left(2(r - r_j) + h_{j+1}\right)/h_{j+1}^3, & r_j \le r \le r_{j+1} \\ 0, & \text{otherwise} \end{cases} \tag{7.5}$$

and

$$\psi_j^b(r) = \begin{cases} (r - r_j)(r - r_{j-1})^2/h_j^2, & r_{j-1} \le r \le r_j \\ (r - r_j)(r_{j+1} - r)^2/h_{j+1}^2, & r_j \le r \le r_{j-1} \\ 0, & \text{otherwise.} \end{cases} \tag{7.6}$$

We will now construct the actual element space V_h with our base vectors. It will consist of vector types

$$(\varphi_i, 0, 0), (\phi_i, 0, 0), (0, \varphi_i, 0), (0, \phi_i, 0), (0, 0, \psi_i^a) \text{ and } (0, 0, \psi_i^b).$$

The first two types correspond to u, the second two to θ and the last two to w. The order of the vector in $\mathbf{N}$ can be freely chosen, but we have chosen to arrange them as follows:

For each $k \in \{0, \ldots, m\}$

$$\begin{aligned} \mathbf{N}_k &= (\varphi_k, 0, 0)^T \\ \mathbf{N}_{k+1} &= (\phi_k, 0, 0)^T \\ \mathbf{N}_{k+2} &= (0, \varphi_k, 0)^T \\ \mathbf{N}_{k+3} &= (0, \phi_k, 0)^T \\ \mathbf{N}_{k+4} &= (0, 0, \psi_k^a)^T \\ \mathbf{N}_{k+5} &= (0, 0, \psi_k^b)^T \end{aligned} \tag{7.7}$$

The size of $\mathbf{N}$ is now $3 \times 6(m+1)$, where $h = 1/m$ is the mesh size. The matrix $\mathbf{A}$ will be of the size $6(m+1) \times 6(m+1)$. However, it is both sparse and symmetric. The arrangement of $\mathbf{N}$ ensures that $\mathbf{A}_{ij} = 0$ when $|i-j| > 12$.

Now the load $\mathbf{q} = (0, 0, \delta)$ so that

$$\int_\omega \mathbf{q}\,\mathbf{N}\,\mathrm{d}\omega = (0, 0, 1, 0, \ldots, 0).$$

Since the elements are at most of degree three we can calculate the corresponding integrals accurately. We could use Gauss' quadrature or other numerical methods, too. We shall use Matlab to do the numerical calculations. We choose $t = 0.01$, $R = 3$, $k = 1/3$, $\nu = 1/3$ and $L = 1$. We give m the values 5, 10, 100 and 500. The different approximations for w are given below in Figure 7.1. The exact solution can also be seen in the Figure. We note that there is a small spike near the origin, see Figure 7.2. It corresponds to the term $t^2 \log r$ in the exact solution. We see that even small values of m give good approximations for our problem. Hence, $p = 3$ was enough to prevent locking. Near the origin, when $r \approx \sqrt{t}$ we see that if $1/m > \sqrt{t}$ we get incorrect results. We can adapt our method so that we refine our mesh near the origin, for example, when $r \leq 2\sqrt{t}$. This would be necessary if we needed large m even to get correct results when r is large. Let the size of the matrix be $n = 6 * (m+1)$ where $m+1$ is the number of the mesh points. Without adaptation $m = 1/h$. If we had a refinement, say, $x_i - x_{i-1} = h$, $i \leq N$ and $x_i - x_{i-1} = 4h, i > N$ we would get

$$n = \frac{1}{4}(\frac{1}{h} + 3N).$$

If further

$$N = 2\frac{\sqrt{t}}{h} = \frac{1}{5h},$$

then $m = \frac{2}{5h} < \frac{1}{h}$ so that that the size of the matrix is smaller. The amount of work needed to invert this kind of matrix is $\mathcal{O}(n)$ (see [GHG86]). Hence, we would save some time by this adaptation if we needed very large m to get correct results. However, our problem is nicely solved even for $m = 100$ so there is really no need for special refinement.

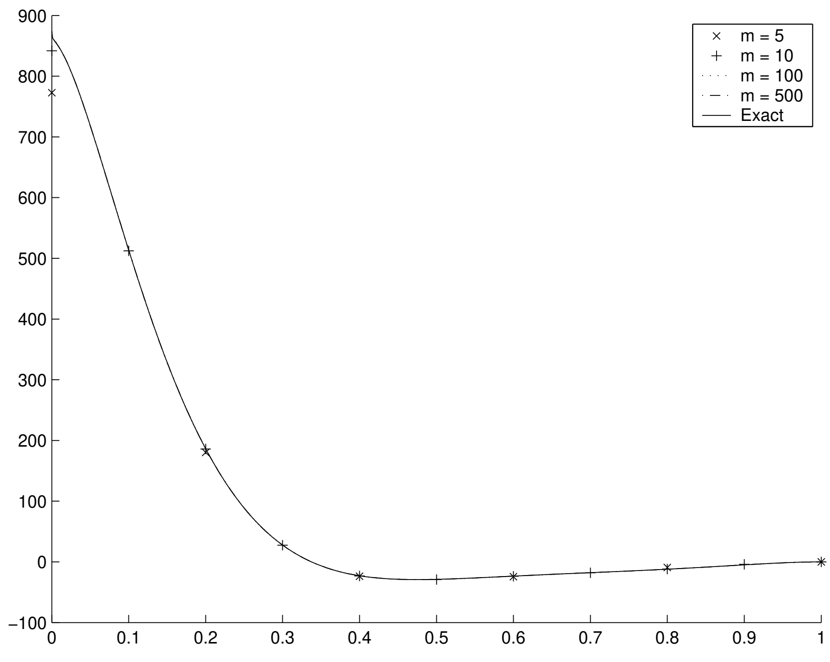

Figure 7.1: Naghdi: The cases $m = 5$, $m = 10$, $m = 100$, $m = 500$ and the exact solution

7.2 Koiter

Let us first construct the matrices **S** and **D** for Koiter as we did for Naghdi in the previous Section. The membrane matrices are

$$\mathbf{S}_\beta = \begin{pmatrix} \frac{d}{dr} & \frac{1}{R} \\ \frac{1}{r} & \frac{1}{R} \end{pmatrix} \ \mathbf{D}_\beta = \begin{pmatrix} 1 & \nu \\ \nu & 1 \end{pmatrix} \tag{7.8}$$

and the bending matrices are

$$\mathbf{S}_\kappa = \begin{pmatrix} 0 & \frac{d^2}{dr^2} \\ 0 & \frac{1}{r}\frac{d}{dr} \end{pmatrix} \ \mathbf{D}_\kappa = \frac{t^2}{12} \begin{pmatrix} 1 & \nu \\ \nu & 1 \end{pmatrix}. \tag{7.9}$$

Now $\mathbf{u} \in \mathrm{H}_0^1 \times \mathrm{H}_0^1$ so that linear elements defined in equation (7.4) should suffice for both u and w. However, a linear w means that the solution near the origin is singular. Then we should demand that $\varphi_0 = 0$ so that $w = 0$ in the origin but this is not the real solution.

We can circumvent the problem by increasing the degree of the space V_h such that we will use cubic elements for w. They were defined in equations (7.5) and (7.6). The linear elements will still suffice for u. The matrix **N** of size $2 \times 3(m + 1)$ will be constructed in a similar way to Naghdi in Section 7.1:

For each $k \in \{0, \ldots, m\}$

$$\begin{aligned} \mathbf{N}_k &= (\varphi_k, 0) \\ \mathbf{N}_{k+1} &= (0, \psi_k^a) \\ \mathbf{N}_{k+2} &= (0, \psi_k^b). \end{aligned} \tag{7.10}$$

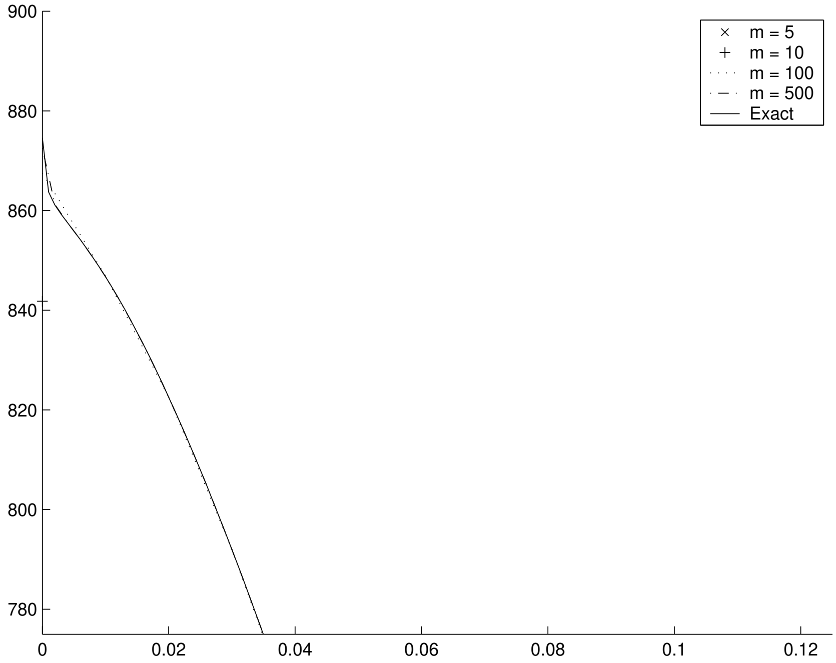

Figure 7.2: Naghdi near the Origin

We can see that the size of $\mathbf{A}$ is $3(m+1) \times 3(m+1)$. The load vector will be

$$\mathbf{b} = \int_{\omega} \mathbf{q}\,\mathbf{N}\,\mathrm{d}\omega = (0, 1, 0, \ldots, 0).$$

The numerical solution is calculated with Matlab. We have used the same numerical values for parameters as in Section 7.1: $t = 0.01$, $R = 3$, $\nu = 1/3, k = 1/3, L = 1$ and $m = 5, 10, 100$ and 500. The approximations for w for different m are shown in Figure 7.3 with the exact solution. The solution near the origin is in Figure 7.4. We see that in this case there is no spike near the origin as there was in Figure 7.2. This is consistent with our exact solution in Chapter 5 since there was no singular term in w.

In Figure 7.5 both Naghdi and Koiter with $m = 100$ are shown. In this scale there can be seen no difference between the two models. In Figure 7.6 we get a closer look at the two solutions near the origin. Here we can see that Koiter is limited finite, whereas Naghdi has a “spike” near the origin. Our numerical results are then coincident with the exact solutions, see also Table 8.1. Similarly to the previous Section, since there is no locking anymore, we could improve our solution simply by refining the solution near the origin. Since the problem can be solved nicely with only $m = 100$ there is no need for adaptation.

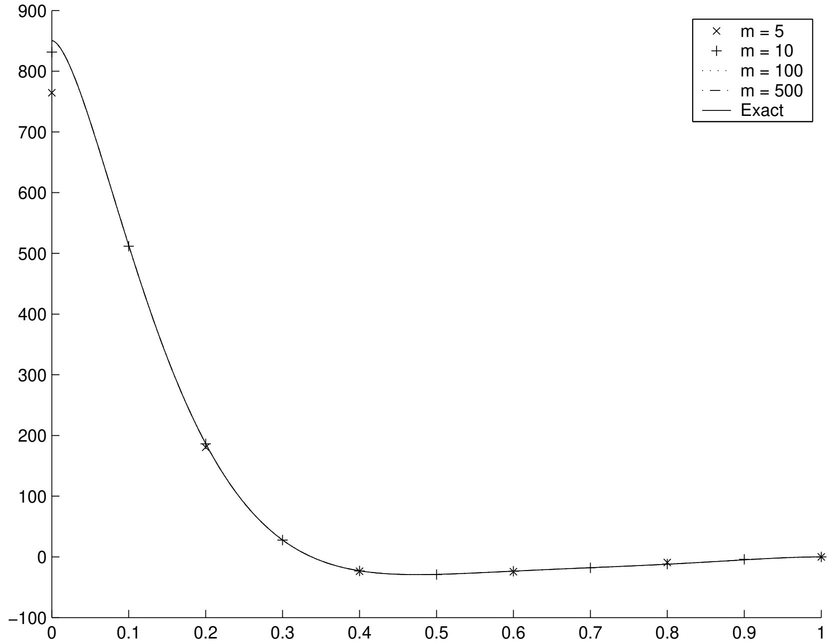

Figure 7.3: Koiter: Cases $m = 5, m = 10, m = 100, m = 500$ and the exact solution.

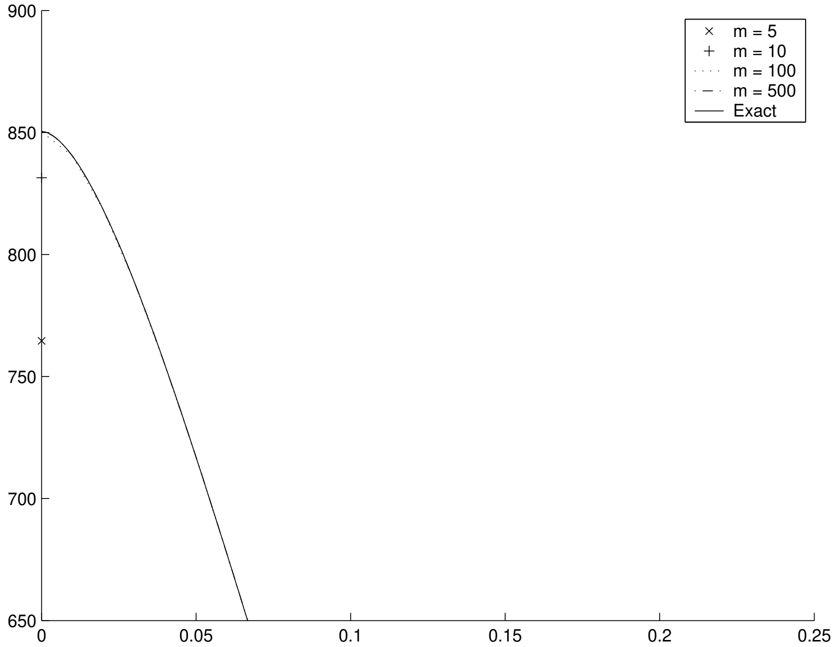

Figure 7.4: Koiter near the origin

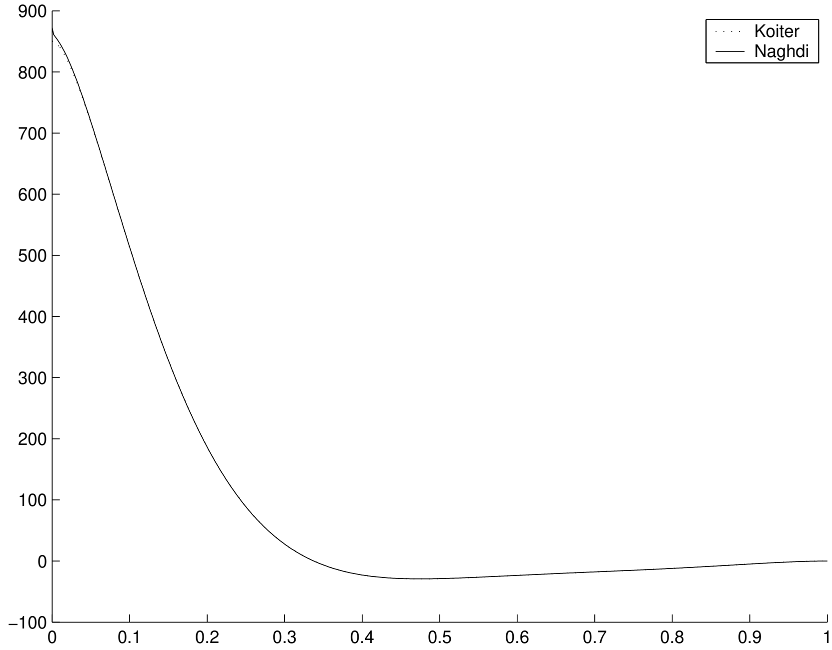

Figure 7.5: Koiter and Naghdi with $m = 100$

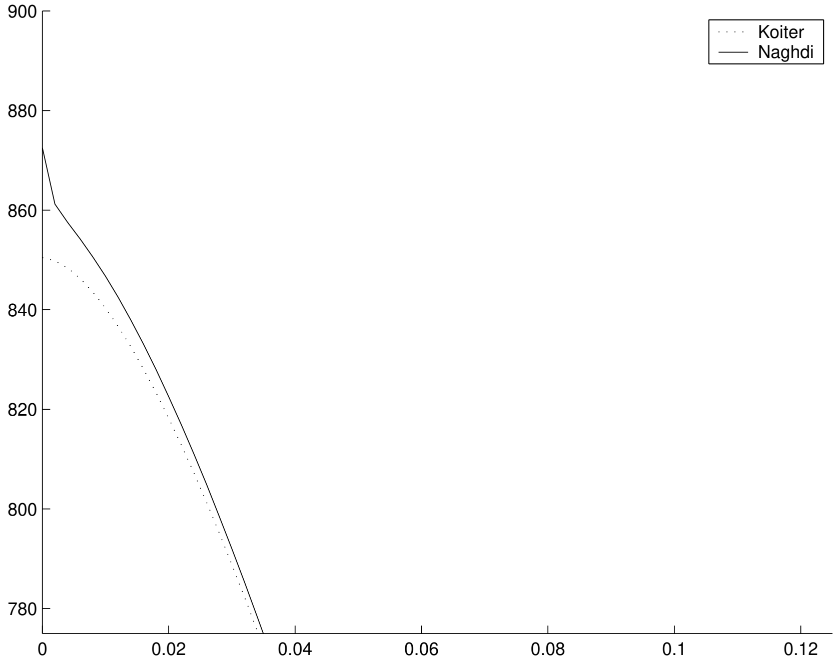

Figure 7.6: Koiter and Naghdi near the origin with $m = 100$

Chapter 8

Conclusions

In this thesis an important benchmark problem for shallow shells was studied. The problem consisted of a spherical shell under a concentrated load. With a non-symmetric load the problem would have been three-dimensional. However, in this work the load was concentrated at the origin so that the problem became one-dimensional. The boundary conditions were also chosen to be symmetric: The shell was clamped on the edges and hence, it could not move. The main interest laid in the normal deflection, i.e., the deformation to the direction of the normal of the shell, since it describes best the behaviour of the shell. For completeness, the tangential and angular deformations were solved as well.

In this Chapter the results will be analyzed. The next Section concentrates on the differences and similarities between the solutions of the different models.

8.1 Comparison of the different models

In Chapter 3 we studied the two plate models, Reissner-Mindlin and Kirchhoff. In Chapter 4 the membrane theory was studied. It can be seen as a "simplified" version of Koiter model, the classical shell model that was solved in Chapter 5. Finally, we studied the modern shell problem, Naghdi's model, in Chapter 6.

We are mostly interested in what happens near the origin, since the deflections are largest there. In Table 8.1 below, the results for the different models near the origin are presented.

We have also examined the behaviour of the object near the boundary, and the corresponding values are in the Table 8.2. We are now going to analyze the differences as well as the similarities between the different solutions. This might help us to understand the behaviour of the plates and shells more profoundly. It might also help to solve more complex cases since we – if we are lucky – may be able to simplify a shell to a plate, for example.

Model	w	θ
Kirchhoff	$\frac{3}{2\pi t^2} r^2 \ln r$	$w' \approx \frac{3}{\pi t^2} r \ln r$
Reissner-Mindlin	$\frac{1}{2\pi k} \ln r + \frac{3}{2t^2\pi} r^2 \ln r$	$\frac{3}{\pi t^2} r \ln r$
Membrane	$\frac{1}{2\pi(\nu - 1)} + \frac{R^2}{\pi(1-\nu)\epsilon^2}$	
Koiter	$\frac{3}{2\pi} r^2 \ln r$	$w' \approx \frac{3}{\pi} r^2 \ln r$
Naghdi	$\frac{t^2}{2\pi k} \ln r + \frac{3}{2\pi} r^2 \ln r$	$\frac{t^2}{4\pi k} \hat{p}(\hat{b} + \frac{R2\sqrt{3}k}{t^2\sqrt{1-\nu^2}}) r \ln r$

Table 8.1: The deflections for different models near the origin

Model	w	θ
Kirchhoff	$\frac{3}{2\pi t^2}\left(r^2 \ln \frac{r}{L} + \frac{L^2 - r^2}{2}\right)$	$w' = \frac{3}{\pi t^2} r \ln \frac{r}{L}$
Reissner-Mindlin	$\frac{3}{2t^2\pi}\left(r^2 \ln \frac{r}{L} + \frac{L^2 - r^2}{2}\right)$	$\frac{3}{t^2\pi} r \ln \frac{r}{L}$
Membrane	$\frac{R^2}{1-\nu^2}\delta$	
Koiter	$e^{\frac{\alpha(r-L)}{\sqrt{2}}} f,\ f = \mathcal{O}(1)$	$w' \approx e^{\frac{\alpha(r-L)}{\sqrt{2}}} g,\ g = \mathcal{O}(1)$
Naghdi	$e^{-\frac{\hat{p}L}{\sqrt{2t}} r} f,\ f =$trig,	$e^{-\frac{\hat{p}L}{\sqrt{2t}} r} g,\ g =$trig

Table 8.2: The deflections for different models near the boundary

The membrane theory differs from the others in that it has a partially defined load instead of a concentrated load. It has no shell thickness parameter. It can be seen to be derived from the Koiter's model by putting $t = 0$. We saw that the Koiter's model behaved similarly when we were far from the origin, i.e., the load. This is because the bending stresses are negligible there. Near the load the bending energy becomes significant and the membrane theory is not applicable.

The Kirchhoff and Reissner-Mindlin models for plates were studied in Chapter 3. From Table 8.1 we see that when the thickness parameter t is small, the two models coincide near the origin. However, if t cannot be considered negligible, the normal deflections of the models differ by the term

$$t^2 \ln r$$

which a is part of the Reissner-Mindlin model's solution. Far from the origin, near the boundary, the two models coincide, as can be seen from Table 8.2.

The rotation θ is also similar in the two cases, where in the classical model $\theta = w'$. The difference is again of the order t^2 compared to the similar terms and far from the origin there is no difference between the two rotations.

The differences of the two shell models were similar to the differences of the two plate models. The normal deflection in Naghdi's model, as well as in the Reissner-Mindlin's model, has the term

$$t^2 \ln r$$

which is not present in the Koiter's model. This is negligible when t is small. When $r \approx L$ the Naghdi and Koiter models coincide again, as can be seen in Table 8.2.

We see that there is no essential difference between plates and shells when r is near the origin. This can be justified from the fact that when r is small, we have the approximation $\frac{r}{R} \ll 1$. Now this can be interpreted as $R \approx \infty$ for shells. As noted in Chapter 2, $R = \infty$ for plates. Hence, near the origin, the shells look like plates and behave similarly. (Compare what the world looks like when you stand on the ground to looking it from the space).

The differences between the classical and the modern models is the shearing energy: There is no shearing strain in Koiter's or Kirchhoff's models. We also have no real rotation to be solved since it is simply w'. The equations are then of fourth degree (see Section 2.6) and the logarithmic term cannot rise (see Theorem 2.4.) Then, as can be assumed in the classical model, the energy is bounded.

When the shearing strain is added we will also have $w' \neq \theta$. The non-homogeneous equations we obtained for Reissner-Mindlin and Naghdi (see equations (3.13) and (6.3), respectively) were of second degree. Hence, the distributive solution had the logarithmic term in it and the corresponding shearing energy was not bounded anymore.

The differences and similarities depend on the ratios of r, t and R, i.e., they depend mainly on the thickness of the shell and the location we are on the shell. Near the origin the shell can be approximated by the plate, at least in symmetric cases. Far from the origin the Koiter's model can be approximated by the membrane theory.

Finally, we wanted to solve our problem with Finite Element Method. We constructed the method for our problem and then solved both Naghdi's and Koiter's models. The results were shown in Chapter 7. Our numerical solutions coincided with our analytical solutions described above. Our problem would have locked if the elements spaces had been chosen incorrectly. However, since we had to choose elements of high degree, we could not see the locking in action. On the other hand, we could see the dominating layer's effect on our solution.

8.2 Next step

This work concentrated on the spherical, polar symmetric case. If the load was non-symmetric, for example, the problem could be a two- or three-dimensional. Then it should first be simplified to one dimension by Fourier transformation. After this the one-dimensional methods could be tried to be applied to the problem. The problem could also be complicated by making the shell non-symmetric, i.e., by choosing an ellipsoid or maybe a cylinder instead of a sphere.

In these cases the mathematical problem is tried to be returned to one dimension. The FEM would be done in the problem's original dimension so that it would be two- or maybe even three-dimensional. Then the effects of locking and dominating layers may be seen even better. Finally it should be noted that if the problem is made too complex, an analytic solution will be impossible to find and one must be satisfied with numerical solutions. To this end, the benchmark problem of this work gives a good idea on the way the more complex problem would behave under FEM.

Appendix A

Table of notations and abbreviations

Notation	**Meaning**	**See page**
FEM	Finite Element Method	46
ber, bei, ker, kei	Kelvin functions	27
$\hat{w}$	Fourier transform of w	30
J_0, Y_0, J_1, Y_1	Bessel functions	36
$\|\| \cdot \|\|_m$	Sobolev-norm	13
$\mathcal{A}$	quadratic part of the energy	8
$\mathcal{F}$	energy	8
$\mathcal{G}$	linear elastic operator	20
$\mathcal{L}$	linear differential operator	13
$\mathbf{A}$	stiffness matrix	15
$\mathbf{S}_\beta, \mathbf{D}_\beta, \mathbf{S}_\kappa, \mathbf{D}_\kappa,$ $\mathbf{S}_\rho, \mathbf{D}_\rho$	membrane, bending and strain matrices for FEM	46, 49
(b_{ij})	curvature tensor	6
$\mathbf{b}$	load vector	15
$\mathbf{e}_n$	normal of the shell	4
$\mathbf{e}_1, \mathbf{e}_2$	tangengial vectors of the shell	7
$\mathbf{f}(\mathbf{u})$	external forces	9
$\mathbf{q}$	traction	9
$\mathbf{u} = (u, v, w, \theta, \phi)$	deformation of the shell	6
$\mathbf{u}_h$	approximate solution	15
Γ, Γ_0	the middle surface	4
Ω	domain of the shell	4
β_{ij}	membrane strain tensor	7
γ	shear correction factor	8
δ	δ-distribution	14
θ	angular deformation	6
κ_{ij}	bending strain tensor	7
ν	Poisson's ratio	8
ρ_{ij}	shear strain tensor	8

ϕ	angular deformation (used only in Chapter 2)	6
ϕ_i	element polynomial of second degree (used only in Chapter 7)	47
φ_i^h	(general) element functions	16
φ_i	element polynomial of first degree	47
ξ	variable on Fourier side	30
ψ_i^a	element polynomial of third degree	47
ψ_i^b	element polynomial of third degree	47
ω	other parametrization for middle surface	5
A_i	Lamé's coefficients	5
H^m	Sobolev space	12
L	radius of plate, radius of projection	4
R	radius of curvature	4
$a(\mathbf{u}, \mathbf{v})$	membrane (and shearing) energy	8
$b(\mathbf{u}, \mathbf{v})$	bending energy	9
e	error for finite element method	11
h	(maximum) mesh spacing	16
$k = \frac{1}{2}\gamma(1-\nu)$		8
m	mesh density	16
n	layer mode/scale	12
t	thickness of a shell	4
r, φ	variables on ω	5
u, v	tangential deformations	6
w	normal deformation	6
x_i	shell's coordinates	4

Bibliography

[Eva98] Laurence C. Evans. *Partial Differential Equations.* Providence (RI): American Mathematical Society, first edition, 1998.

[GHG86] Charles F. van Loan Gene H. Golub. *Matrix Computations.* North Oxford Academic Publishers Ltd., first edition, 1986.

[HH96] J. Pitkäranta H. Hakula, Y. Leino. Scale resolution, locking, and high-order finite element modelling of shells. *Comput. Methods App. Mech. Engrg.*, pages 157–182, 1996.

[JP01] C. Shwab J. Pitkäranta, A.-M. Matache. Fourier mode analysis of layers in shallow shell deformations. *Comput. Methods App. Mech. Engrg.*, pages 2943–2975, 2001.

[LR99] Bertil Westergren Lennart Råde. *Mathematics Handbook for Science and Engineering.* Studentlitteratur, third edition, 1999.

[Łuk79] Stanislaw Łukasiewicz. *Local loads in plates and shells.* PWN-Polish Scientific Publishers, first edition, 1979.

[MA65] Irene A. Stegun Milton Abramowitz. *Handbook of Mathematical Functions.* National Bureau of Standards, fourth edition, 1965.

[Nov59] V.V. Novozhilov. *The theory of thin shells.* Groningen: Noordhoff, first edition, 1959.

[Rud91] Walter Rudin. *Functional Analysis.* McGraw-Hill, second edition, 1991.